American Journal of Human Biology

Obstetric dimensions of the female pelvis are less integrated than locomotor dimensions and show protective scaling patterns: Implications for the obstetrical dilemma

Journal:	*American Journal of Human Biology*
Manuscript ID	AJHB-20-0003.R2
Wiley - Manuscript type:	Original Research Article
Date Submitted by the Author:	n/a
Complete List of Authors:	Ricklan, Sarah; University of Cambridge; New York University School of Medicine Decrausaz, Sarah-Louise; University of Cambridge; University of Victoria Wells, Jonathan; UCL Great Ormond Street Institute of Child Health Stock, Jay; University of Cambridge; Western University; Max Planck Centre for the Science of Human History
Keywords:	obstetrical dilemma, obstetric, integration, pelvis, phenotypic plasticity

Title:

Obstetric dimensions of the female pelvis are less integrated than locomotor dimensions and show protective scaling patterns: Implications for the obstetrical dilemma

Running title:

Obstetric and locomotor scaling and integration

Authors:

Sarah J. Ricklan[1,2] (corresponding author)
Sarah-Louise Decrausaz[1,3]
Jonathan C.K. Wells[4]
Jay Stock[1,5,6]

Institutional affiliation:

[1]Department of Archaeology, University of Cambridge

Current address

[2] New York University Grossman School of Medicine, New York NY, USA, Sarah.Ricklan@nyulangone.org
[3] Department of Anthropology, University of Victoria
[4] UCL Great Ormond Street Institute of Child Health, London, UK
[5] Department of Anthropology, Western University, London, Ontario, Canada
[6] Department of Archaeology, Max Planck Centre for the Science of Human History, Jena, Germany

Abstract:

Objectives: The 'obstetrical dilemma' hypothesis assumes that the modern human female pelvis serves two discrete functions: obstetrics and locomotion. We investigate whether these differing functions create observable patterns of morphological covariation and whether those patterns differ by height, weight, age. This allows evaluation of evidence for canalization and phenotypic plasticity relevant to obstetric and locomotor function among a living female population.

Methods: Landmarks (N=86) were collected and inter-landmark distances were calculated (N=36) on the pelvis and proximal femur of CT scans of living women aged 20 to 90 years (M=93) receiving a routine CT scan. Partial least squares and relative standard deviation of eigenvalues analyses were used to evaluate integration overall and within locomotor and obstetric modules, respectively. Ordinary Least Squared regression was used to evaluate scaling relationships between inter-landmark distances and height, weight, and age.

Results: The obstetric pelvis was significantly less internally integrated than the locomotor pelvis. Many obstetric measurements were constrained in absolute terms relative to height; shorter women had relatively larger birth canal dimensions, and several key obstetric dimensions showed relative freedom from height. Lower weight women had some relatively larger obstetric and locomotor dimensions. Regarding age, younger women showed a few relatively larger outlet dimensions.

Conclusions: This study suggests that the obstetric pelvis and the locomotor pelvis function are morphologically distinct, with the obstetric pelvis showing relatively greater flexibility. These

relationships between relative constraints support the hypothesis that the modern female pelvis shows evidence of both canalization and phenotypic plasticity in obstetric and locomotor structures.

Key words:

Obstetrical dilemma; obstetric; integration; pelvis; phenotypic plasticity

Introduction

Researchers often describe the modern human female pelvis as a compromise between the dimensions required for successful childbirth and those required for upright posture and energetically efficient bipedal locomotion (Fischer & Mitteroecker, 2015; Washburn, 1960). Washburn provided a classic conceptualization of this interaction in his phrase "the obstetric dilemma" (OD), by which women experience difficult childbirth today because postural and obstetrical considerations came into conflict in human evolutionary history (Washburn, 1960). Critics argue that the notion of a uniform human OD across populations fails to satisfactorily explain the relationship between difficult childbirth today and the way the human female pelvis evolved (Dunsworth, Warrener, Deacon, Ellison, & Pontzer, 2012; Gruss, Gruss, & Schmitt, 2017; Rosenberg & Trevathan, 1995; Wall-Scheffler & Myers, 2017; Walrath, 2003; Warrener, 2017; Warrener, Lewton, Pontzer, & Lieberman, 2015; Wells, DeSilva, & Stock, 2012; Whitcome, Miller, & Burns, 2017). Further, wide variation in pelvic dimensions exists across populations (reviewed in Betti, 2017; Betti & Manica, 2018), and is influenced by many factors (Auerbach, King, Campbell, Campbell, & Sylvester, 2018; Betti, 2017; Betti, von Cramon-Taubadel, Manica, & Lycett, 2014). Indeed, instead of being a static problem brought about during our evolutionary history, the OD may change with ecological factors such as growth during development and current nutritional status (Wells, 2015; Wells et al., 2012; Wells, Wibaek, & Poullas, 2018). For example, pelvic dimensions of nulliparous South Asian women were found to correlate with tibia length (Shirley, Cole, Arthurs, Clark, & Wells, 2019), a marker of environmental conditions in early life (Whitley, Gunnell, Davey Smith, Holly, & Martin, 2008).

This study contextualizes obstetric and locomotor constraints in the pelvis, the relationship between them, and the factors associated with these patterns in a living sample of human women from a single population. Understanding these relative constraints and freedoms can reveal whether the obstetric and locomotor pelves form separate functional units and can further reveal whether and under what circumstances obstetric function is protected relative to locomotor function. This study focuses on the pubis, which is highly sexually dimorphic (Bilfeld et al., 2015; Patriquin, Loth, & Steyn, 2003; Scheuer & Black, 2000, p. 349) and changes its form significantly during ontogeny (Bilfeld et al., 2015; Scheuer & Black, 2000, p. 349).

To describe pelvic covariation, this study investigates morphological integration and allometry. Integration examines how traits covary, often revealing a shared functional purpose or developmental origin (Willmore, Young, & Richtsmeier, 2007). Individual traits in highly integrated systems have relatively low variation (Pavlicev, Cheverud, & Wagner, 2009). Morphological integration may also be considered in relation to canalization, which buffers the development of traits from environmental and genetic disruptions, and phenotypic plasticity, where changes in response to environmental variation (Willmore et al., 2007) are characterized by increased phenotypic variation (Kurki, 2013, 2017). Canalization and phenotypic plasticity can be evaluated by examining variation in trait integration. Allometric relationships are a form of integration (Armbruster, Pélabon, Bolstad, & Hansen, 2014) and their comparison is appropriate for analyzing pelvic integration.

Few previous studies have evaluated human pelvic integration. Those that have compared human and nonhuman primate integration have found conflicting results (Grabowski, 2013; Grabowski, Polk, & Roseman, 2011; Lewton, 2012). Mallard, Savell, and Auerbach (2017) did not examine the effect of height and weight on integration but found moderate pelvic integration in a modern archaeological population, with no difference in integration or variance across age groups. The pubis, which continues to grow into a woman's twenties (Rissech & Malgosa, 2007) and thirties (Tague, 1994), with parts growing until age 35 to 40 (Scheuer & Black, 2000, p. 371; Verbruggen & Nowlan, 2017), does not grow out of proportion to the rest of the pelvis (Mallard et al., 2017). Mallard et al. (2017) found the outlet to be the most integrated part of the pelvis, suggesting higher integration for obstetric measurements. However, since integration reduces variability (Willmore et al., 2007), more highly integrated systems should show lower levels of variation, and the pelvic canal is the most variable region of the pelvis (Candelas González, Rascón Pérez, Chamero, Cambra-Moo, & González Martín, 2017; Kurki, 2013; Kurki & Decrausaz, 2016). Given these non-intuitive results, a comparison of obstetric and locomotor integration is warranted.

Studies that have examined pelvic variation with height in humans and non-human primates have presented diverse results in the pelvis. Some studies suggest that pelvic dimensions do not correlate with height (Kurki, 2011a, 2013; Takamuku, 2019; Wood & Chamberlain, 1986), while others found correlations in certain dimensions (Jagesur, Wiid, Pretorius, Bosman, & Oettlé, 2017; Lewton, 2015; Mobb & Wood, 1977; Sharma, Gupta, & Shandilya, 2016; Tague, 2000). Certain pubic measurements did show correlation (Jagesur et al.,

2017) and allometric scaling with height (Mobb & Wood, 1977). Similarly diverse results have been presented regarding the relationship between pelvic obstetric dimensions and weight, with some dimensions showing independence from weight (Tague, 2000), and others, including birth canal size, correlating with weight (Kurki, 2011a; Tague, 2000), body width (Kurki, 2013; Tague, 2000), or body size (Kurki, 2007; Sharma et al., 2016). In addition, correlations between pubic measurements and weight have been documented (Rosenberg, 1988; Young, Johannesdottir, Poole, Shaw, & Stock, 2018). Other analyses have examined the relationship of locomotor measurements such as femoral head diameter (Ruff, Scott, & Liu, 1991; Young et al., 2018) and femoral neck width (Ruff et al., 1991) with weight. Studies that have examined the scaling relationships between pelvic measurements and adult age may suggest that the female pelvis is largest among skeletally mature younger adults (Berger, May, Renner, Viradia, & Dahners, 2011; Huseynov et al., 2016), and obstetric and locomotor regions of the pelvis may grow at different rates (Moerman, 1982; Sharma et al., 2016). The above discussion highlights substantial variation in reported relationships between pelvic and body size measures.

Although the studies described above have investigated how pelvis dimensions relate to height, weight, and age, no previous studies have examined how obstetric and locomotor measurements vary with respect to these factors and to each other. This study expands on the work of Mallard et al. (2017), who evaluated integration and allometry in obstetric and locomotor measurements of the pelvis, and evaluating the effects of height, weight, and age.

Materials and Methods

Pelvic CT scans were obtained from a previous study (Poole et al., 2010) evaluating femoral neck structure in (n=100) healthy female volunteers aged 20 to 90 years visiting

Addenbrooke's Hospital in Cambridge, UK for a routine clinical CT scan unrelated to skeletal disease. Scans consisted of the lower portion of the pelvis and did not include the full ilium or sacrum. Poole et al. (2010) received ethical approval for their study from the Cambridgeshire Regional Ethics Committee; study participants were recruited according to the Declaration of Helsinki. All images were anonymized, and bone structural analysis was undertaken according to the conditions of participant informed consent via a material transfer agreement between medicine and anthropology. The sample for this study (N=93) was a subset of the sample described by Poole et al. (2010). Although participants' ethnic ancestry information was not available, the sample represents a predominantly white British population.

Using Avizo Fire version 6.3.1, landmarks were placed on each of 93 3D surface images reconstructed from DICOM files containing 3D CT scan data. 44 landmarks on the pelvis and proximal femur were chosen (Table S2). Forty-two were collected bilaterally; two (MP4, along the sacrum between the fourth and fifth vertebrae, and STIP, the sacral tip) were midline landmarks. A total of 86 landmarks were collected. 36 inter-landmark distances were calculated (Table 1), which were chosen because of their relevance to obstetrics (landmarks: N = 19 per side, and N = 2 midline; inter-landmark distances: N = 21) and locomotion (landmarks: N = 23 per side; inter-landmark distances N = 15). They were selected if they were found in published literature analyzing pelvic morphology, traced musculature related to obstetrics or locomotion, or provided focused analysis of the pubis.

The landmarks and inter-landmark distances were divided into two categories, "obstetric" and "locomotor." Obstetric measurements were defined as measurements related to the bony birth canal and measurements following muscle attachments or bony structures impacted by pregnancy and/or childbirth. General internal measurements of the pubis were also taken and classified as obstetric. Some measurements examined general pelvic dimensions without following muscle attachments or the bony birth canal; internal (medial) landmarks or measures related to pubic breadth that may be affected by pregnancy and delivery were classified as obstetric. Locomotor measurements were defined as measurements following or related to muscle attachments of walking, as well as measurements of the acetabulum and proximal femur. Additionally, general ventral measurements of the pubis were taken and classified as locomotor because of their proximity to locomotor muscle attachments. To check whether these divisions were appropriate, a correlation matrix of the inter-landmark distances was constructed, and correlation coefficients analyzed using R version 3.4.2 (R Core Team, 2017) and version 3.6.2 (R Core Team, 2019) software package *corrplot* version 0.84 (Wei & Simko, 2017) (Fig. 1) (Olson & Miller, 1958), an R function (STHDA), and Microsoft Excel for Mac version 16.34. The absolute values of the correlations were overall higher among locomotor (mean 0.45; median 0.40; minimum 0.12; maximum 0.88) and obstetric measurements (mean 0.32; median 0.26; minimum 0.03; maximum 0.88) than between them (mean 0.31; median 0.31; minimum 0.08; maximum 0.59). This suggested that obstetric and locomotor measurements may form two internally integrated units. The divisions into obstetric and locomotor categories therefore represented divisions into two true groups that could then be compared in subsequent analysis.

Using R version 3.4.2 (R Core Team, 2017) software package *geomorph* version 3.0.6 (Adams, Collyer, & Kaliontzopoulou, 2018), inter-landmark distances were calculated (32 bilaterally, four represented distances from left to right); a total of 68 distances were calculated. For bilateral inter-landmark distances, the average of left- and right-side measurements were calculated to produce a final set of 36 inter-landmark distances. Estimates of missing landmarks were not used to calculate inter-landmark distances. R code is available upon request.

A full set of landmarks was collected twice by the same investigator (SJR) on ten randomly chosen CT scans. To evaluate error in landmark coordinate collection, landmarks were processed as described below (with 17 total missing landmarks) paired t-tests were performed on landmark coordinate data (based on Barbeito-Andrés, Anzelmo, Ventrice, & Sardi, 2012). Wilcoxon Signed-Rank tests were used when normality assumptions were not met based on Shapiro-Wilk tests. If only one variable of a pair showed a non-parametric distribution, both paired t-tests and Wilcoxon Signed-Rank tests were performed. These results were compared, and a decision was made about the error. To check error in inter-landmark distance calculation, the full set of inter-landmark distances was calculated using the landmarks that were collected for a second time. A total of 46 inter-landmark distances were unable to be calculated due to missing landmarks. Paired t-tests were used to evaluate whether there was a difference in means between the original inter-landmark distance measurements and the new measurements (Decrausaz, 2014). Wilcoxon Signed-Rank tests were used as above.

Integration

To evaluate integration between obstetric and locomotor measurements using landmarks, the R version 3.4.2 (R Core Team, 2017) software package *geomorph* version 3.0.6 (Adams et al., 2018) was used. The Thin-Plate Spline method (Fischer & Mitteroecker, 2015, 2017), was used, with a complete reference specimen, to estimate missing landmarks (137 missing landmarks in the whole pelvis, all but two specimens with 6 or fewer missing landmarks; one specimen had 20 and another had 33 missing landmarks) (Gunz, Mitteroecker, Neubauer, Weber, & Bookstein, 2009). A Generalized Procrustes Analysis (GPA) was then performed to standardize the landmarks. An integration test using a two-block partial least squares analysis was performed (reviewed in Klingenberg, 2014) comparing obstetric and locomotor landmarks for left and right sides independently (each including midline landmarks MP4 and STIP), as well as for the whole pelvis. The same analysis was performed for landmarks contained in the pubis alone (obstetric: N = 11 per side, locomotor: N = 8 per side; 16 missing landmarks in the whole pubis, one specimen with 2 missing and 1 with 14 missing).

Following Mallard et al. (2017), patterns of integration among inter-landmark distances were analyzed, first analyzing overall pelvic integration among all inter-landmark distances and then integration among inter-landmark distances related to obstetrics and integration among inter-landmark distances related to locomotion. To standardize the data, inter-landmark distances were transformed using natural logarithms. Individuals with one or more missing inter-landmark distance were omitted, leaving 66 complete measurement sets. The method proposed by Pavlicev et al. (2009) was used. A correlation matrix was constructed, and eigenvalues were calculated for the matrix. Each eigenvalue represents the amount of variance in its eigenvector, and a larger difference between eigenvalues represents a higher level of integration (Pavlicev et al., 2009). When positive, negative, and mixed-sign correlations appear in a correlation matrix, the relative standard deviation of the eigenvalues ($SD_{rel}(\lambda)$) is an appropriate measure of the differences between them, and therefore is a measure of integration (Pavlicev et al., 2009). This method accounts for the number of measurements (inter-landmark distances) used to construct each correlation matrix, so integration can be compared regardless of matrix size (Pavlicev et al., 2009).

Following Mallard et al. (2017) and Pavlicev et al. (2009), relative standard deviation of eigenvalues was calculated using the following equation:

$$SD_{rel}(\lambda) = \frac{\sqrt{Var(\lambda)}}{\sqrt{N-1}},$$

where $\boldsymbol{\lambda}$ equals the eigenvalue and N equals the number of inter-landmark distances. Var($\boldsymbol{\lambda}$) was calculated using the following equation:

$$Var(\lambda) = \frac{\sum_{i=1}^{N}(\lambda_i - 1)^2}{N},$$

where N is the number of inter-landmark distances, and $\boldsymbol{\lambda}_i$ is the ith eigenvalue. Using the *boot* library version 1.3-20 (Canty & Ripley, 2017; Davison & Hinkley, 1997) in R version 3.4.2 (R Core Team, 2017), and following Mallard et al. (2017), an adjusted bootstrap 95% confidence interval for $SD_{rel}(\boldsymbol{\lambda})$ was calculated using the normal approximation using bootstrapping with replacement over 10,000 iterations. This method of bootstrapping assumes a normal distribution. This method corrects for bias between the bootstrapped mean and the calculated value, and it centers the confidence interval around (2 x $SD_{rel}(\boldsymbol{\lambda})$ - mean(t), where t represents the bootstrapped estimates. Calculated $SD_{rel}(\boldsymbol{\lambda})$ values were compared to the conservative estimate of $SD_{rel}(\boldsymbol{\lambda})$ without integration that Mallard et al. (2017) use, $\sqrt{\frac{1}{\frac{M}{2}}}$, where M is the sample size.

Deviating from Mallard et al. (2017), to compare between groups with different values of $\sqrt{\frac{1}{\frac{M}{2}}}$, $SD_{rel}(\boldsymbol{\lambda})$ and bootstrapped confidence intervals were scaled by dividing $SD_{rel}(\boldsymbol{\lambda})$ and confidence intervals by the $\sqrt{\frac{1}{\frac{M}{2}}}$ values for that group. By doing this, an unintegrated scaled $SD_{rel}(\boldsymbol{\lambda})$ was always equal to one. Calculated $SD_{rel}(\boldsymbol{\lambda})$ and confidence intervals could then be compared in relation to this value.

The above procedure was repeated to evaluate the association of height, weight, and age with integration by examining the differences in $SD_{rel}(\boldsymbol{\lambda})$ between women below the median and above the median height (1.62 m), weight (69.9 kg), and age (54.5 years), respectively. The above analyses were also performed for those inter-landmark distances contained only in the pubis (total: N=11; obstetric: N = 5; locomotor: N = 6).

Some $SD_{rel}(\boldsymbol{\lambda})$ values fell outside of their bootstrapped confidence intervals. This can occur when the bootstrapped estimates show a bias relative to the calculated estimate, such that the calculated estimate is offset from the bootstrapped mean. This is possible because the calculated $SD_{rel}(\boldsymbol{\lambda})$ is only an estimate, and it is statistically possible for a bootstrapped mean to differ from it. While the bootstrap method accounts for this bias, it does not always fully compensate for it. When this occurs, one can center the bootstrap mean at the calculated $SD_{rel}(\boldsymbol{\lambda})$, but this was not performed in this study because failure to include the calculated $SD_{rel}(\boldsymbol{\lambda})$ was not considered problematic. The bias may also exist because $SD_{rel}(\boldsymbol{\lambda})$ is always positive (Haber, 2011). In several cases, $SD_{rel}(\boldsymbol{\lambda})$ was higher than the unintegrated threshold, but this was not the case if 95% confidence intervals were taken into account. Mallard et al. (2017) did not use confidence intervals but compared the magnitude of $SD_{rel}(\boldsymbol{\lambda})$ to the unintegrated threshold. In this study, all results will be reported.

In division into smaller groups, confidence intervals sometimes included the unintegrated threshold. The difference between the calculated $SD_{rel}(\boldsymbol{\lambda})$ and the mean calculated by the bootstrap determines the point about which the confidence interval is centered. When there is a bias between the calculated $SD_{rel}(\boldsymbol{\lambda})$ and the mean calculated by the bootstrap, the bootstrapped confidence intervals can be centered either above or below $SD_{rel}(\boldsymbol{\lambda})$, depending on the direction of the bias. If the bias is large enough, the confidence intervals can include the unintegrated threshold. This may have occurred in these smaller group divisions.

Allometric and scaling relationships

Allometric and scaling relationships were evaluated using the R version 3.4.2 (R Core Team, 2017) software package *smatr* version 3.4-8 (Warton, Duursma, Falster, & Taskinen, 2012). Following (Lewton, 2015), the natural logarithms of inter-landmark distances, height, weight, and age were calculated. To correct for the association of height with weight, the same allometric analysis was performed using body mass index (BMI). This was performed using the R version 3.6.2 (R Core Team, 2019), *geomorph* version 3.2.1 (Adams, Collyer, & Kaliontzopoulou, 2020), and *smart* version 3.4-8 (Warton et al., 2012).

Allometric relationships can be calculated using an Ordinary Least Squared (OLS) regression or a Reduced or Standardized Major Axis (SMA) regression (Lewton, 2015). In this study, both methods were performed and were corrected for multiple tests, but only OLS results were interpreted (Lewton, 2015; Smith, 2009; Warton, Wright, Falster, & Westoby, 2006). The regression lines for those variables that correlated significantly with one another were examined to determine whether their slopes were significantly different from one (isometry). Outliers may have weighted the regression analysis, but they were not removed because they represented biological variation in the sample.

Results

Demographic information about study participants can be found in Table S1. Outliers were not excluded.

We first tested for intra-observer error. Results showing significant intra-observer error are displayed in Table S3. Integration tests involving landmark analysis were run again excluding landmarks that showed significant intra-observer error in two dimensions on the same side. Only results excluding these landmarks are discussed. Three inter-landmark distances were measured with significant intra-observer error: two measurements following the levator ani, ISP to BISPA ($p = 0.014$) and ISP to LSCI ($p = 0.008$), and the proximal-distal femoral head diameter, FHPROX to FHD ($p = 0.021$). To include as many inter-landmark distances as possible, the differences in means between measuring bouts of individual sides (rather than the average of left and right sides) were evaluated for these three measurements. The right-side measurement of ISP to LSCI did not show intra-observer error ($p = 0.075$), and so was included in analysis. Because one set of measures showed a normal distribution and the other did not, both a paired t-test and a Wilcoxon Signed-Rank test were used to evaluate the difference between the left-side measurements of ISP to LSCI. The Wilcoxon Signed-Rank test showed no intra-observer error ($p = 0.064$), but the measurement was excluded because the paired t-test showed intra-observer error ($p = 0.040$).

Next, we tested obstetric and locomotor integration overall. Only results from scaled integration analysis will be discussed. The pelvis overall was integrated ($SD_{rel}(\boldsymbol{\lambda}) = 1.454$, where unintegrated $SD_{rel}(\boldsymbol{\lambda}) = 1$) (Table 2), as was the pubis (Table 4). Looking at obstetric and locomotor measurements separately, a partial least squares integration test suggested that the two sets of measurements were integrated with each other within the pelvis (whole pelvis: rPLS = 0.955, $p = 0.007$; right: rPLS = 0.773, $p = 1 \times 10^{-4}$; left: rPLS = 0.798, $p = 2 \times 10^{-4}$). Within the pubis, a partial least squared test suggested that obstetric and locomotor landmarks were integrated with each other (both sides: rPLS = 0.954, $p = 2 \times 10^{-4}$; right: rPLS = 0.965, $p = 1 \times 10^{-4}$; left: rPLS = 0.972, $p = 1 \times 10^{-4}$).

In the overall sample, obstetric ($SD_{rel}(\boldsymbol{\lambda}) = 1.523$ CI 1.241 to 1.546) and locomotor ($SD_{rel}(\boldsymbol{\lambda}) = 1.987$ CI 1.705 to 2.060) measurements were integrated (Table 3). Locomotor measurements were more highly integrated than obstetric measurements, and their confidence intervals did not overlap (Figure 2a). Pubic locomotor measurements were integrated, but although obstetric $SD_{rel}(\boldsymbol{\lambda})$ was higher than it would have been if unintegrated, the lower boundary of the 95% confidence interval was lower. Pubic locomotor measurements were more highly integrated than obstetric measurements (Table 5, Figure 2b). In summary, locomotor measurements were significantly more highly integrated than were obstetric measurements.

We then examined integration within subsets of the data. Importantly, integration was lower in the subsets than it was in the larger sample. This may be caused by bias between the bootstrapped estimate and the calculated estimate when groups were analyzed separately, as confidence intervals widen with smaller sample sizes. This suggests that the integration results derived from the subsets may be less reliable than those from the whole sample.

We then examined integration with respect to height, weight, and age, and found similar results. There were no significant differences in overall pelvic, obstetric, or locomotor integration among the height, weight, and age groups (Table 2). Among height groups, locomotor measurements were not more integrated than obstetric measurements (Table 3, Fig. 3a). With respect to weight groups, the pattern of integration differed slightly. In lower weight women, the confidence intervals of obstetric and locomotor measurements barely overlapped (obstetric CI 0.768 to 1.060; locomotor CI 1.058 to 1.429) (Table 3, Fig. 5a), while in higher weight women, the confidence intervals overlapped (obstetric CI 0.902 to 1.232; locomotor CI 1.090 to 1.517). Similarly, with regard to age groups, although there was no difference in obstetric or locomotor integration between the groups, the pattern differed slightly. In younger women, the confidence intervals of obstetric and locomotor integration overlapped (Table 3, Fig. 7a), but in older women, locomotor measurements were more highly integrated than obstetric measurements. There was no difference in pubic integration among height, weight, or age groups

(Table 4, 5, Fig. 3b, Fig. 5b, Fig. 7b). Pubic locomotor measurements were more highly integrated than pubic obstetric measurements in both height and weight groups. Among age groups, pubic locomotor measurements were more highly integrated than pubic obstetric measurements in older but not younger women.

Significant negative allometric and isometric relationships between inter-landmark distances and height are shown in Table 6, and some relationships between inter-landmark distances and height are displayed in Figure 4. Of 21 obstetric inter-landmark distances, 13 correlated significantly with height. Of these, seven were measures of the birth canal, and these seven scaled with negative allometry. Three of five pubic obstetric measurements correlated with height, while no pubic locomotor measurements correlated with height. The birth canal measurements failing to correlate significantly with height were midplane mediolateral width (ISP to ISP), mid-plane posterior (ISP to MP4), and transverse outlet (INFT to INFT).

Significant negative allometric relationships between inter-landmark distances and weight are shown in Table 7, and some of the relationships between inter-landmark distances and weight are displayed in Figure 6. Of 21 obstetric inter-landmark distances, nine correlated significantly with weight. Three of these were related to the birth canal, while six were unrelated to the birth canal. All obstetric measurements that correlated with weight scaled with negative allometry. Four of five pubic obstetric measurements correlated with weight, and all scaled with negative allometry. The only obstetric pubic inter-landmark distance that did not correlate with weight was PUBR to PUBT. One pubic locomotor measurement correlated with weight.

To account for the association of height with weight in allometric relationships, scaling with BMI was evaluated. Only two measurements scaled with BMI. The pelvic outlet antero-posterior diameter, IPS to STIP, scaled with negative allometry with a slope of 0.078 (CI 0.007

to 0.148) and R^2 of 0.056. This measurement also scaled with negative allometry with height and weight. A measure of the medial inferior pubic ramus, MSIPR to MIIPR, scaled with negative allometry with a slope of 0.154 (CI 0.004 to 0.303) and R^2 of 0.047. This measurement scaled isometrically with height and with negative allometry with weight.

Significant scaling relationships found between inter-landmark distances and age are shown in Table 8, and some are shown in Figure 8. Of 21 obstetric inter-landmark distances, five correlated significantly with age. Three of these were birth canal measurements. One of five pubic obstetric measurements correlated with age (pubic symphysis height, SPS to IPS), and it scaled negatively. No locomotor measurements in the pubis correlated with age.

Discussion

This study examined whether the covariation between the obstetric and the locomotor pelves in a living female population showed patterns of canalization, patterns of phenotypic plasticity, or both. Canalization and plasticity are opposites but may co-occur within a system such as the pelvis. For further evaluation, we studied the variables associated with this covariation. We accomplished this through a study of integration and allometry (Figures 9 and 10) in the pelvis.

Our key finding was that, although the pelvis as a whole represented an integrated unit, the obstetric pelvis was less internally constrained than the locomotor pelvis. This assertion is consistent with findings showing that obstetric measurements, in particular dimensions of the pelvic canal, showed high variability and consequently low constraints (Kurki, 2013; Kurki & Decrausaz, 2016). Additionally, obstetric measurements in the pubis showed a high degree of relative internal freedom and related more strongly to external parameters of growth and nutritional status than did pubic locomotor measurements. A limitation of this study, however, is that the data does not include the entire pelvis but rather only a portion of it. This limitation may affect integration results, particularly with respect to locomotion.

The extent to which obstetric and locomotor integration and measurements are associated with other biometric variables such as height, weight, and age remains an important consideration. Importantly, integration results among subsets of women were less reliable than results for the sample as a whole. Obstetric dimensions were slightly although not significantly less constrained internally in shorter women, suggesting protective flexibility in obstetric dimensions. In other words, obstetric measurements may be allowed to expand more freely in shorter women (Kurki, 2011a) to compensate for an otherwise small skeletal size. In addition, shorter women had relatively larger birth canals and locomotor dimensions, while non-canal obstetric measurements increased in constant proportion with height. These findings carry implications for modern obstetric ease. At an individual level, most obstetric evidence suggests that shorter women experience a higher frequency of cephalopelvic disproportion (Liselele, Boulvain, Tshibangu, & Meuris, 2000; Mahmood, Campbell, & Wilson, 1988; Tsu, 1992) and caesarean section (Mahmood et al., 1988; Sheiner, Levy, Katz, & Mazor, 2005; Toh-Adam, Srisupundit, & Tongsong, 2012; Wells, 2017), even if secular trends of increasing height are associated with greater frequency of caesarean section worldwide (Zaffarini & Mitteroecker, 2019). Since height factors into obstetric ease, allometric patterns, too, should account for height, especially among populations with small-statured mothers (Takamuku, 2019).

However, the nature of these allometric patterns is not straightforward. We found that most birth canal dimensions, including all antero-posterior and anterior birth canal measurements, scaled with negative allometry with respect to height (Figure 9). This suggests that shorter women had larger birth canal dimensions relative to their stature compared to taller women. Of all the obstetric dimensions to correlate with height, midplane anterior (IPS to ISP) showed the highest correlation, scaling with negative allometry. However, three dimensions of the birth canal did not correlate with height: midplane medio-lateral width (ISP to ISP), mid-plane posterior (ISP to MP4), and transverse outlet (INFT to INFT). Another measure of outlet mediolateral width, INN to INN, correlated with height, but weakly compared to other birth canal dimensions.

Our results suggest that the midplane and outlet face a combination of relative constraints in antero-posterior and anterior dimensions and relative freedom in mediolateral and posterior dimensions relative to height. This may allow for greater flexibility, or ability to change, in the latter dimensions (Kurki, 2011a). The midplane, particularly midplane medio-lateral width (ISP to ISP), is the narrowest portion of the birth canal, and is therefore considered the most obstetrically critical dimension (reviewed in Kurki, 2011a). Indeed, in modern obstetrics, women who experienced obstructed labor had narrower midplane medio-lateral dimensions than women with unobstructed labor (Frémondière, Thollon, Adalian, Delotte, & Marchal, 2017; Zaretsky et al., 2005). Additionally, women with obstructed labor showed contraction in the anterior-posterior dimension (Frémondière et al., 2017; Zaretsky et al., 2005), the longest dimension of the midplane (Rosenberg, 1992). Turning now to the outlet, another key measure of pelvic contraction is outlet medio-lateral width (Kurki, 2011a). Transverse outlet diameter may correlate with obstructed labor, as may contraction in the anterior-posterior outlet (Frémondière et al., 2017). Therefore, some but not all of the tightest dimensions of the midplane and outlet showed relative freedom from height, while those that are more accommodating to the fetal head and shoulders showed greater constraints.

There was a weak relationship between weight and integration. Lower weight women had slightly but not significantly lower obstetric and locomotor integration than did higher weight women. In the pubis, lower weight women showed a magnitude of integration suggesting a lack of integration, while higher weight women did not; while not significant, this might point to relatively greater freedom in the pubis in lower weight women. Measurements were less constrained allometrically relative to weight than they were to height, but lower weight women had relatively larger obstetric and locomotor dimensions (Figure 10). Few measurements correlated with weight, supporting Ruff et al. (1991) and Young et al. (2018), including only three birth canal measurements, suggesting that these dimensions were relatively larger in lower weight women. Regarding non-canal measurements, while only the height of the pubic symphysis correlated with body height, both the width and the height of the pubic symphysis scaled with negative allometry with weight, suggesting that lighter women had relatively larger pubic symphysial dimensions. Similarly, within the pubis, almost all obstetric measurements scaled with negative allometry with weight, in contrast to Rosenberg (1988), who found that heavier populations had relatively longer pubic bones.

To evaluate whether our weight and height findings influenced each other, since shorter women may also have had lower weights, we examined scaling with BMI. However, only two measurements, both obstetric, correlated with BMI, and both did so weakly. This suggests that the study participant's current physique or nutrition explains little of the variability found in this study. It further suggests that the allometric relationships we found with weight may actually be driven by relationships with height. However, the large age range we studied is a limitation to this conclusion. In contrast, pelvic dimensions have been shown to be correlated to maternal

BMI in a Brazilian cohort, and explained the association of BMI with neonatal size (Wells, Figueiroa, & Alves, 2017).

Our findings regarding age support Mallard et al. (2017), who found that integration did not change across age groups. In the pubis, however, while obstetric measurements were slightly integrated in younger women, the magnitude of integration in older women suggests a lack of integration. Further, there was a significant difference in integration between obstetric and locomotor measurements in older women but not in younger women. These findings may suggest that pubic obstetric developmental coordination may relax once growth is complete, as some parts of the pubis grow until age 35 to 40 (Scheuer & Black, 2000, p. 371; Verbruggen & Nowlan, 2017). Most measurements were comparatively unconstrained relative to age. Some outlet measures scaled with age, suggesting that younger women had relatively larger outlet dimensions. This may represent secular trends or changes over a lifetime as proposed by Huseynov et al. (2016), who reported that female obstetric measurements, particularly in the outlet, were smaller and more male-like in older compared to younger women. In terms of modern obstetrics, high maternal age has been associated with greater risk of cephalopelvic disproportion (Tsu, 1992). This obstetrical finding might be explained in part by decreasing obstetric dimensions with age, although increasing BMI with age as well as increased infant size with maternal age and parity may play a larger role. In addition, non-birth canal obstetric measurements also showed a decrease in proportional relationship with age. In particular, pubic symphysis height showed the highest correlation, aligning well with developmental evidence that the pubic symphysis continues to grow into early mid-life (Scheuer & Black, 2000, p. 371; Verbruggen & Nowlan, 2017). It further suggests that this relative growth decreases with age.

The contrast in relative constraints and freedoms between obstetric and locomotor measurements is notable, and our findings validate the hypothesis that the obstetric and locomotor pelves can be considered two functional units that also interact and overlap. The combination of relative freedom and constraints acting differently on the obstetric and locomotor pelves may be approached through a lens of phenotypic plasticity and canalization. Integration, and therefore allometry, can be understood as a constraining force (reviewed in Armbruster et al., 2014) because it limits the amount of possible variation (Willmore et al., 2007) and thus limits the potential for change. In a similar way, canalization limits the amount of variation in a system (Willmore et al., 2007). While integration and canalization are not identical, they can both act on the same system to similar effect (Willmore et al., 2007).

Our results suggest that obstetric traits show plasticity; however, it is important to recognize that canalization of some traits may also explain these results. The variation found between obstetric dimensions and between key obstetric measurements and height could be interpreted as a result of developmental canalization to compensate for more plastic biometric traits such as linear growth and nutritional status. In this light, it would be informative to determine whether obstetric measurements are indeed canalized throughout development to allow for a minimum obstetric pelvic size to facilitate childbirth regardless of other biometry, or whether these key obstetric measurements in fact change relatively freely with respect to body size.

This study does not reveal whether the forces acting upon the pelvis are environmental or genetic, if either, but environmental influences may be substantial. In this light, the environment can influence pelvic measurements though mechanisms of phenotypic plasticity. Wells et al. (2012) have suggested that such environmental, particularly nutritional, effects have exacerbated childbirth difficulties by simultaneously reducing maternal pelvic dimensions and increasing fetal dimensions. They argue that neonatal body mass and maternal height show phenotypic plasticity, although the mother may buffer neonatal body mass against external environmental stresses (Wells, 2015; Wells et al., 2012), as neonatal size shows a correlation with maternal pelvic dimensions (Wells et al., 2017). If phenotypic plasticity is characterized by increased variation (Kurki, 2013, 2017), as is lack of integration (Willmore et al., 2007), the lack of integration we found with respect to obstetric measurements may represent underlying phenotypic plasticity.

Biometric patterns can expand our understanding of the relationship between body size and pelvic plasticity. We found that some of the tightest birth canal measurements were relatively unconstrained relative to height. Phenotypic plasticity, as represented by the lack of constraint relative to height, would be particularly favorable in shorter women. However, our results also suggest that many dimensions of the obstetric pelvis may be canalized with respect to height, suggestive of common regulatory mechanism in skeletal growth. Further, as discussed above, the lack of allometric relationships and integration may actually represent some developmental canalization to ensure adequate pelvic size. Similarly, with respect to weight, while few obstetric measurements were constrained in association with this variable, those that were scaled with negative allometry, such that lower weight women had larger obstetric dimensions, suggesting possible canalization in these metrics with potential for plasticity in others. Integration may also be lower in lower weight women, particularly in the pubis. These patterns suggest that lower weight women might also benefit from phenotypic plasticity in certain obstetric regions. In the modern era, however, rising obesity produces larger neonates, exacerbating difficulty in childbirth (Wells, 2017). Today, women of higher weights may benefit more from phenotypic plasticity than would women of lower weights. The pattern of relative freedoms and constraints we found may further exacerbate modern obstetric complications (sensu Wells, 2017). Since short stature and increased weight may be risk factors (both independently and taken together) (Wells et al., 2018), the interplay between freedoms and constraints should be further elucidated to understand the modern obstetric dilemma.

Our study strongly suggests that there are differences between the obstetric pelvis and the locomotor pelvis. The obstetric dilemma model has provided a useful suggestion that may carry implications for medical policy: obstetric and locomotor dimensions serve as two functional modules within the pelvis. Even if the modern human female pelvis does not represent a compromise between the obstetric and locomotor pelvis, the obstetric and locomotor modules of the pelvis are individually identifiable. Understanding the dynamics of pelvic constraint and freedom can reveal how modern female pregnancy and parturition can change in the long- and the short-term.

Acknowledgements:

The authors would like to acknowledge Dr. Ken Poole for providing access to his CT scan database that formed the data set for this study. The authors would like to acknowledge Dr. Laura Buck and Dr. Jaap Saers for technical and logistical support and Dr. Enrico Crema and Dr. Erik Gjesfjeld for their advice regarding statistical analysis.

Author contributions:

SJR collected and analyzed the data and drafted the manuscript. SJR, SLD, JCKW and JTS designed the study and revised the manuscript.

References

Adams, D. C., Collyer, M. L., & Kaliontzopoulou, A. (2018). Geomorph: Software for geometric morphometric analyses. R package version 3.0.6. https://cran.r-project.org/package=geomorph.

Adams, D. C., Collyer, M. L., & Kaliontzopoulou, A. (2020). Geomorph: Software for geometric morphometric analyses. R package version 3.2.1, https://cran.r-project.org/package=geomorph.

Armbruster, W. S., Pélabon, C., Bolstad, G. H., & Hansen, T. F. (2014). Integrated phenotypes: understanding trait covariation in plants and animals. *Philosophical Transactions of the Royal Society of London B, 369*, 20130245-20130245. doi:10.1098/rstb.2013.0245

Auerbach, B. M., King, K. A., Campbell, R. M., Campbell, M. L., & Sylvester, A. D. (2018). Variation in obstetric dimensions of the human bony pelvis in relation to age-at-death and latitude. *American Journal of Physical Anthropology, 167*(3), 628-643. doi:10.1002/ajpa.23690

Barbeito-Andrés, J., Anzelmo, M., Ventrice, F., & Sardi, M. L. (2012). Measurement error of 3D cranial landmarks of an ontogenetic sample using Computed Tomography. *Journal of Oral Biology and Craniofacial Research, 2*, 77-82. doi:10.1016/J.JOBCR.2012.05.005

Berger, A. A., May, R., Renner, J. B., Viradia, N., & Dahners, L. E. (2011). Surprising evidence of pelvic growth (widening) after skeletal maturity. *Journal of Orthopaedic Research, 29*(11), 1719-1723. doi:10.1002/jor.21469

Betti, L. (2017). Human variation in pelvic shape and the effects of climate and past population history. *The Anatomical Record, 300*, 687-697. doi:10.1002/ar.23542

Betti, L., & Manica, A. (2018). Human variation in the shape of the birth canal is significant and geographically structured. *Proceedings of the Royal Society B, 285*(1889). doi:10.1098/rspb.2018.1807

Betti, L., von Cramon-Taubadel, N., Manica, A., & Lycett, S. J. (2013). Global geometric morphometric analyses of the human pelvis reveal substantial neutral population history effects, even across sexes. *PLOS ONE, 8*, e55909-e55909. doi:10.1371/journal.pone.0055909

Betti, L., von Cramon-Taubadel, N., Manica, A., & Lycett, S. J. (2014). The interaction of neutral evolutionary processes with climatically-driven adaptive changes in the 3D shape of the human os coxae. *Journal of Human Evolution, 73*, 64-74. doi:10.1016/j.jhevol.2014.02.021

Bilfeld, M. F., Dedouit, F., Sans, N., Rousseau, H., Rougé, D., & Telmon, N. (2015). Ontogeny of size and shape sexual dimorphism in the pubis: a multislice computed tomography study by geometric morphometry. *Journal of Forensic Sciences, 60*, 1121-1128. doi:10.1111/1556-4029.12761

Candelas González, N., Rascón Pérez, J., Chamero, B., Cambra-Moo, O., & González Martín, A. (2017). Geometric morphometrics reveals restrictions on the shape of the female *os coxae*. *Journal of Anatomy, 230*, 66-74. doi:10.1111/joa.12528

Canty, A., & Ripley, B. D. (2017). boot: Bootstrap R (S-Plus) Functions.

Davison, A. C., & Hinkley, D. V. (1997). *Bootstrap Methods and Their Applications*. Cambridge: Cambridge University Press.

Decrausaz, S.-L. (2014). *A morphometric analysis of partuition scarring on the human pelvic bone.* (Master of Arts). University of Victoria.

Dunsworth, H. M., Warrener, A. G., Deacon, T., Ellison, P. T., & Pontzer, H. (2012). Metabolic hypothesis for human altriciality. *Proceedings of the National Academy of Sciences of the United States of America, 109*, 15212-15216. doi:10.1073/pnas.1205282109

Fischer, B., & Mitteroecker, P. (2015). Covariation between human pelvis shape, stature, and head size alleviates the obstetric dilemma. *Proceedings of the National Academy of Sciences of the United States of America, 112*, 5655-5660. doi:10.1073/pnas.1420325112

Fischer, B., & Mitteroecker, P. (2017). Allometry and sexual dimorphism in the human pelvis. *The Anatomical Record, 300*, 698-705. doi:10.1002/ar.23549

Frémondière, P., Thollon, L., Adalian, P., Delotte, J., & Marchal, F. (2017). Which foetal-pelvic variables are useful for predicting caesarean section and instrumental assistance? *Medical Principles and Practice, 26*, 359-367. doi:10.1159/000477732

Grabowski, M. W. (2013). Hominin obstetrics and the evolution of constraints. *Evolutionary Biology, 40*, 57-75. doi:https://doi.org/10.1007/s11692-012-9174-7

Grabowski, M. W., Polk, J. D., & Roseman, C. C. (2011). Divergent patterns of integration and reduced constraint in the human hip and the origins of bipedalism. *Evolution, 65*, 1336-1356. doi:10.1111/j.1558-5646.2011.01226.x

Gray, H. (1918). *Anatomy of the human body* (20th ed ed.). Philadelphia: Lea & Febiger.

Gruss, L. T., Gruss, R., & Schmitt, D. (2017). Pelvic breadth and locomotor kinematics in human evolution. *The Anatomical Record, 300*, 739-751. doi:10.1002/ar.23550

Gunz, P., Mitteroecker, P., Neubauer, S., Weber, G. W., & Bookstein, F. L. (2009). Principles for the virtual reconstruction of hominin crania. *Journal of Human Evolution, 57*, 48-62. doi:10.1016/J.JHEVOL.2009.04.004

Haber, A. (2011). A comparative analysis of integration indices. *Evolutionary Biology, 38*, 476-488. doi:10.1007/s11692-011-9137-4

Huseynov, A., Zollikofer, C. P. E., Coudyzer, W., Gascho, D., Kellenberger, C., Hinzpeter, R., & Ponce de León, M. S. (2016). Developmental evidence for obstetric adaptation of the human female pelvis. *Proceedings of the National Academy of Sciences of the United States of America, 113*, 5227-5232. doi:10.1073/pnas.1517085113

Jagesur, S., Wiid, A., Pretorius, S., Bosman, M. C., & Oettlé, A. C. (2017). Assessment of the variability in the dimensions of the intact pelvic canal in South Africans: a pilot study. *HOMO - Journal of Comparative Human Biology, 68*, 30-37. doi:10.1016/j.jchb.2016.11.003

Klingenberg, C. P. (2014). Studying morphological integration and modularity at multiple levels: concepts and analysis. *Philosophical Transactions of the Royal Society B, 369*, 20130249-20130249. doi:10.1098/rstb.2013.0249

Kurki, H. K. (2007). Protection of obstetric dimensions in a small-bodied human sample. *American Journal of Physical Anthropology, 133*, 1152-1165. doi:10.1002/ajpa.20636

Kurki, H. K. (2011a). Compromised skeletal growth? Small body size and clinical contraction thresholds for the female pelvic canal. *International Journal of Paleopathology, 1*, 138-149. doi:10.1016/j.ijpp.2011.10.004

Kurki, H. K. (2011b). Pelvic dimorphism in relation to body size and body size dimorphism in humans. *Journal of Human Evolution, 61*, 631-643. doi:10.1016/J.JHEVOL.2011.07.006

Kurki, H. K. (2013). Skeletal variability in the pelvis and limb skeleton of humans: does stabilizing selection limit female pelvic variation? *American Journal of Human Biology, 25*, 795-802. doi:10.1002/ajhb.22455

Kurki, H. K. (2017). Bilateral asymmetry in the human pelvis. *The Anatomical Record, 300*, 653-665. doi:10.1002/ar.23546

Kurki, H. K., & Decrausaz, S.-L. (2016). Shape variation in the human pelvis and limb skeleton: implications for obstetric adaptation. *American Journal of Physical Anthropology, 159*, 630-638. doi:10.1002/ajpa.22922

Lewton, K. L. (2012). Evolvability of the primate pelvic girdle. *Evolutionary Biology, 39*, 126-139. doi:10.1007/s11692-011-9143-6

Lewton, K. L. (2015). Allometric scaling and locomotor function in the primate pelvis. *American Journal of Physical Anthropology, 156*, 511-530. doi:10.1002/ajpa.22696

Liselele, H. B., Boulvain, M., Tshibangu, K. C., & Meuris, S. (2000). Maternal height and external pelvimetry to predict cephalopelvic disproportion in nulliparous African women: a cohort study. *British Journal of Obstetrics and Gynaecology, 107*, 947-952. doi:10.1111/j.1471-0528.2000.tb10394.x

Mahmood, T. A., Campbell, D. M., & Wilson, A. W. (1988). Maternal height, shoe size, and outcome of labour in white primigravidas: a prospective anthropometric study. *BMJ, 297*(6647), 515-517.

Mallard, A. M., Savell, K. R. R., & Auerbach, B. M. (2017). Morphological integration of the human pelvis with respect to age and sex. *The Anatomical Record, 300*, 666-674. doi:10.1002/ar.23547

Mobb, G. E., & Wood, B. A. (1977). Allometry and sexual dimorphism in the primate innominate bone. *American Journal of Anatomy, 150*, 531-538. doi:10.1002/aja.1001500403

Moerman, M. L. (1982). Growth of the birth canal in adolescent girls. *American Journal of Obstetrics and Gynecology, 143*, 528-532. doi:https://doi.org/10.1016/0002-9378(82)90542-7

Olson, E. C., & Miller, R. L. (1958). *Morphological Integration*. Chicago: The University of Chicago Press.

Patriquin, M. L., Loth, S. R., & Steyn, M. (2003). Sexually dimorphic pelvis morphology in South African whites and blacks. *HOMO, 53*, 255-262. doi:https://doi.org/10.1078/0018-442X-00049

Pavlicev, M., Cheverud, J. M., & Wagner, G. P. (2009). Measuring morphological integration using eigenvalue variance. *Evolutionary Biology, 36*, 157-170. doi:10.1007/s11692-008-9042-7

Poole, K. E. S., Mayhew, P. M., Rose, C. M., Brown, J. K., Bearcroft, P. J., Loveridge, N., & Reeve, J. (2010). Changing structure of the femoral neck across the adult female lifespan. *Journal of Bone and Mineral Research, 25*(3), 482-491. doi:10.1359/jbmr.090734

R Core Team. (2017). R: A Language and Environment for Statistical Computing. Vienna, Austria.

R Core Team. (2019). R: A language and environment for statistical computing. R. F. f. S. Computing (Ed.). Vienna, Austria.

Raviv, E. (2015). Adding Text to R Plot. *R-bloggers.* Retrieved from https://www.r-bloggers.com/adding-text-to-r-plot/

Rissech, C., & Malgosa, A. (2007). Pubis growth study: applicability in sexual and age diagnostic. *Forensic Science International, 173*, 137-145. doi:10.1016/J.FORSCIINT.2007.02.022

Rosenberg, K. R. (1988). The functional significance of Neandertal pubic length. *Current Anthropology, 29*, 595-617. doi:10.2307/2743510

Rosenberg, K. R. (1992). The evolution of modern human childbirth. *American Journal of Physical Anthropology, 35*, 89-124. doi:10.1002/ajpa.1330350605

Rosenberg, K. R., & Trevathan, W. (1995). Bipedalism and human birth: the obstetrical dilemma revisited. *Evolutionary Anthropology, 4*, 161-168. doi:10.1002/evan.1360040506

Ruff, C. B., Scott, W. W., & Liu, A. Y. C. (1991). Articular and diaphyseal remodeling of the proximal femur with changes in body mass in adults. *American Journal of Physical Anthropology, 86*, 397-413. doi:10.1002/ajpa.1330860306

Scheuer, L., & Black, S. (2000). *Developmental Juvenile Osteology* (1 ed.). London: Academic Press.

Sharma, K., Gupta, P., & Shandilya, S. (2016). Age related changes in pelvis size among adolescent and adult females with reference to parturition from Naraingarh, Haryana (India). *HOMO - Journal of Comparative Human Biology, 67*(4), 273-293. doi:10.1016/J.JCHB.2016.04.002

Sheiner, E., Levy, A., Katz, M., & Mazor, M. (2005). Short stature - an independent risk factor for cesarean delivery. *European Journal of Obstetrics, Gynecology, and Reproductive Biology, 120*, 175-178. doi:10.1016/j.ejogrb.2004.09.013

Shirley, M. K., Cole, T. J., Arthurs, O. J., Clark, C. A., & Wells, J. C. K. (2019). Developmental origins of variability in pelvic dimensions: Evidence from nulliparous South Asian women in the United Kingdom. *Am J Hum Biol*, e23340. doi:10.1002/ajhb.23340

Smith, R. J. (2009). Use and misuse of the reduced major axis for line-fitting. *American Journal of Physical Anthropology, 140*, 476-486. doi:10.1002/ajpa.21090

STHDA. Correlation matrix: A quick start guide to analyze, format and visualize a correlation matrix using R software. Retrieved from http://www.sthda.com/english/wiki/correlation-matrix-a-quick-start-guide-to-analyze-format-and-visualize-a-correlation-matrix-using-r-software#infos

Tague, R. G. (1994). Maternal mortality or prolonged growth: age at death and pelvic size in three prehistoric Amerindian populations. *American Journal of Physical Anthropology, 95*, 27-40. doi:10.1002/ajpa.1330950103

Tague, R. G. (2000). Do big females have big pelves? *American Journal of Physical Anthropology, 112*, 377-393. doi:10.1002/1096-8644(200007)112:3<377::AID-AJPA8>3.0.CO;2-O

Takamuku, H. (2019). Does obstetric protection apply to small-bodied females?: A comparison between small-bodied Jomon foragers and large-bodied Yayoi agriculturalists in the prehistoric Japanese archipelago. *American Journal of Human Biology, 31*(3), e23236. doi:10.1002/ajhb.23236

Toh-Adam, R., Srisupundit, K., & Tongsong, T. (2012). Short stature as an independent risk factor for cephalopelvic disproportion in a country of relatively small-sized mothers. *Archives of gynecology and obstetrics, 285*(6), 1513-1516. doi:10.1007/s00404-011-2168-3

Tsu, V. D. (1992). Maternal height and age: risk factors for cephalopelvic disproportion in Zimbabwe. *International Journal of Epidemiology, 21*, 941-946. doi:10.1093/ije/21.5.941

Verbruggen, S. W., & Nowlan, N. C. (2017). Ontogeny of the human pelvis. *The Anatomical Record, 300*, 643-652. doi:10.1002/ar.23541

Wall-Scheffler, C. M., & Myers, M. J. (2017). The biomechanical and energetic advantages of a mediolaterally wide pelvis in women. *The Anatomical Record, 300*, 764-775. doi:10.1002/ar.23553

Walrath, D. (2003). Rethinking pelvic typologies and the human birth mechanism. *Current Anthropology, 44*, 5-31.

Warrener, A. G. (2017). Hominin hip biomechanics: changing perspectives. *The Anatomical Record, 300*, 932-945. doi:10.1002/ar.23558

Warrener, A. G., Lewton, K. L., Pontzer, H., & Lieberman, D. E. (2015). A wider pelvis does not increase locomotor cost in humans, with implications for the evolution of childbirth. *PLOS ONE, 10*(3), 1-15. doi:10.1371/journal.pone.0118903

Warton, D. I., Duursma, R. A., Falster, D. S., & Taskinen, S. (2012). smatr 3 - an R package for estimation and inference about allometric lines. *Methods in Ecology and Evolution, 3*, 257-259.

Warton, D. I., Wright, I. J., Falster, D. S., & Westoby, M. (2006). Bivariate line-fitting methods for allometry. *Biological Reviews, 81*, 259-291. doi:10.1017/S1464793106007007

Washburn, S. L. (1960). Tools and human evolution. *Scientific American, 203*, 62-75.

Wei, T., & Simko, V. (2017). R package "corrplot": Visualization of a Correlation Matrix.

Wells, J. C. K. (2015). Between Scylla and Charybdis: renegotiating resolution of the `obstetric dilemma' in response to ecological change. *Philosophical Transactions of the Royal Society B, 370*, 20140067-20140067. doi:10.1098/rstb.2014.0067

Wells, J. C. K. (2017). The new “obstetrical dilemma”: stunting, obesity and the risk of obstructed labour. *The Anatomical Record, 300*, 716-731. doi:10.1002/ar.23540

Wells, J. C. K., DeSilva, J. M., & Stock, J. T. (2012). The obstetric dilemma: an ancient game of Russian roulette, or a variable dilemma sensitive to ecology? *American Journal of Physical Anthropology, 55*, 40-71. doi:10.1002/ajpa.22160

Wells, J. C. K., Figueiroa, J. N., & Alves, J. G. (2017). Maternal pelvic dimensions and neonatal size: implications for growth plasticity in early life as adaptation. *Evolution, Medicine, and Public Health*, 191-200. doi:10.1093/emph/eox016

Wells, J. C. K., Wibaek, R., & Poullas, M. (2018). The Dual Burden of Malnutrition Increases the Risk of Cesarean Delivery: Evidence From India. *Front Public Health, 6*, 292. doi:10.3389/fpubh.2018.00292

Whitcome, K. K., Miller, E. E., & Burns, J. L. (2017). Pelvic rotation effect on human stride length: releasing the constraint of obstetric selection. *The Anatomical Record, 300*, 752-763. doi:10.1002/ar.23551

Whitley, E., Gunnell, D., Davey Smith, G., Holly, J. M., & Martin, R. M. (2008). Childhood circumstances and anthropometry: the Boyd Orr cohort. *Ann Hum Biol, 35*(5), 518-534. doi:10.1080/03014460802294250

Williams, M. B. (2014). *Osteometric phenotypic variation in a collection of pelvic CT scans of a modern female population.* (Master of Philosophy Master’s Thesis). University of Cambridge. Cambridge, UK.

Willmore, K. E., Young, N. M., & Richtsmeier, J. T. (2007). Phenotypic variability: its components, measurement and underlying developmental processes. *Evolutionary Biology, 34*, 99-120. doi:10.1007/s11692-007-9008-1

Wood, B. A., & Chamberlain, A. T. (1986). The primate pelvis: allometry or sexual dimorphism? *Journal of Human Evolution, 15*, 257-263. doi:10.1016/S0047-2484(86)80053-7

Young, M., Johannesdottir, F., Poole, K., Shaw, C., & Stock, J. T. (2018). Assessing the accuracy of body mass estimation equations from pelvic and femoral variables among modern British women of known mass. *Journal of Human Evolution, 115*, 130-139. doi:10.1016/J.JHEVOL.2017.10.011

Zaffarini, E., & Mitteroecker, P. (2019). Secular changes in body height predict global rates of caesarean section. *Proceedings of the Royal Society B: Biological Sciences, 286*(1896), 20182425. doi:10.1098/rspb.2018.2425

Zaretsky, M. V., Alexander, J. M., McIntire, D. D., Hatab, M. R., Twickler, D. M., & Leveno, K. J. (2005). Magnetic resonance imaging pelvimetry and the prediction of labor dystocia. *Obstetrics & Gynecology, 106*, 919-926. doi:10.1097/01.AOG.0000182575.81843.e7

Tables

Table 1: Inter-landmark distances calculated		
Landmark 1	Landmark 2	Rationale†
PEC	LSSPR‡	following pectineus
SPEC	LSSPR‡	following pectineus
PUBR	PUBT§	general pubic breadth measurement that may be affected by pregnancy and parturition (reviewed in Decrausaz, 2014)
PUBC	AIIS§	following rectus abdominus
PMPS	AMPS§	width of pubic symphysis
SPS	IPS§	length of pubic symphysis (Jagesur et al., 2017; Kurki, 2017; Lewton, 2015; Williams, 2014)
IPS	ISP§	midplane anterior (Kurki, 2017)
IPS	INN§	outlet anterior (Kurki, 2017)
IPS	INFT§	outlet anterior (Jagesur et al., 2017; Kurki, 2017)
IPS	MP4§	midplane antero-posterior (Decrausaz, 2014)
IPS	STIP§	pelvic outlet antero-posterior diameter (Decrausaz, 2014; Jagesur et al., 2017; Mallard et al., 2017)
LSSPR	LMSPR‡	following pectineus
LSSPR	LISPR‡	measure of superior pubic ramus
LSIPR	LMIPR‡	following obturator externus
LSIPR	LIIPR‡	measure of inferior pubic ramus
LSIPR	AOF‡	following obturator externus
MSSPR	MISPR§	measure of superior pubic ramus
MSIPR	MIIPR§	measure of inferior pubic ramus
BISPP	ISP§	following levator ani
BISPP	BISPA§	following levator ani
ISP	ISP§	interspinous (midpelvis) diameter; midplane mediolateral width (Decrausaz, 2014; Jagesur et al., 2017; Mallard et al., 2017)
ISP	BISPA§	following levator ani
ISP	LSCI§	following levator ani
ISP	SCI§	after Betti, von Cramon-Taubadel, Manica, and Lycett (2013)
ISP	MP4§	midplane posterior (Decrausaz, 2014; Kurki, 2017; Mallard et al., 2017)
INN	INN§	outlet mediolateral (Decrausaz, 2014; Kurki, 2011a, 2011b; Mallard et al., 2017)
INN	MP4§	outlet posterior (Decrausaz, 2014; Kurki, 2017)
INFT	INFT§	transverse outlet (Jagesur et al., 2017)
POF	AOF‡	obturator antero-posterior diameter (Betti et al., 2013)
ACP	ACA‡	acetabulum antero-posterior diameter (adapted from Lewton, 2015; Williams, 2014)
ACS	ACI‡	acetabulum superior-inferior diameter (adapted from Lewton, 2015; Williams, 2014)

FHPROX	FHD‡	femoral head proximo-distal diameter (adapted from Decrausaz, 2014; Kurki, 2017)
FHA	FHPOS‡	femoral head antero-posterior diameter (adapted from Decrausaz, 2014; Kurki, 2017)
GTT	GTT‡	bitrochanteric breadth (Williams, 2014)
TFD	TFP‡	following obturator externus
NA	NP‡	femoral neck antero-posterior diameter (Williams, 2014)

† Inter-landmark distances related to muscle attachments were defined based on Gray (1918). All other measurements without citations were defined for this study.
‡ Inter-landmark distances classified as locomotor measurements.
§ Inter-landmark distances classified as obstetric measurements.

Table 2. Scaled integration of inter-landmark distances among height, weight, and age groups†

Group	M	Scaled $SD_{rel}(\boldsymbol{\lambda})$	Scaled 95% CI	Scaled $\sqrt{\frac{1}{M/2}}$
All	66	1.454	1.161, 1.471	1
Shorter	25	1.032	0.661, 1.039	1
Taller	36	1.085	0.780, 1.034	1
Lower weight	28	1.101	0.775, 1.090	1
Higher weight	33	1.089	0.772, 1.045	1
Younger	29	1.099	0.741, 1.106	1
Older	34	1.140	0.831, 1.111	1

† The first line represents integration in the whole sample. Each subsequent set of results divides the whole sample into height, weight, and age groups, respectively.

Table 3. Scaled integration of obstetric and locomotor measurements among height, weight, and age groups†

Group	Category‡	M	Scaled $SD_{rel}(\boldsymbol{\lambda})$	Scaled 95% CI	$\sqrt{\frac{1}{M/2}}$
All	Obst.	66	1.523	1.241, 1.546	1
	Loc.	90	1.987	1.705, 2.060	1
Shorter	Obst.	25	1.085	0.721, 1.100	1
	Loc.	40	1.223	0.871, 1.246	1
Taller	Obst.	36	1.182	0.890, 1.157	1
	Loc.	45	1.374	1.076, 1.408	1
Lower weight	Obst.	28	1.086	0.768, 1.060	1
	Loc.	40	1.379	1.058, 1.429	1
Higher weight	Obst.	33	1.215	0.902, 1.232	1
	Loc.	45	1.445	1.090, 1.517	1
Younger	Obst.	29	1.152	0.837, 1.141	1

	Loc.	44	1.437	1.080, 1.502	1
Older	Obst.	34	1.160	0.848, 1.156	1
	Loc.	43	1.509	1.208, 1.569	1

† The first line represents integration in the whole sample. Each subsequent set of results divides the whole sample into height, weight, and age groups, respectively.
‡ Obst. and Loc. represent values calculated after accounting for intra-observer error.

Table 4. Scaled integration of pubic inter-landmark distances among height, weight, and age groups†

Group	M	Scaled $SD_{rel}(\boldsymbol{\lambda})$	Scaled 95% CI	Scaled $\sqrt{\frac{1}{\frac{M}{2}}}$
All	91	1.804	1.473, 1.892	1
Shorter	45	1.258	0.900, 1.276	1
Taller	41	1.332	0.995, 1.403	1
Lower weight	40	1.228	0.871, 1.268	1
Higher weight	46	1.368	1.005, 1.435	1
Younger	44	1.296	0.920, 1.352	1
Older	44	1.357	0.995, 1.432	1

† The first line represents integration in the whole sample. Each subsequent set of results divides the whole sample into height, weight, and age groups, respectively.

Table 5. Scaled integration of pubic obstetric and locomotor measurements among height, weight, and age groups†

Group	Category	M	Scaled $SD_{rel}(\boldsymbol{\lambda})$	Scaled 95% CI	$\sqrt{\frac{1}{\frac{M}{2}}}$
All	Obst.	91	1.392	0.784, 1.716	1
	Loc.	92	2.408	2.109, 2.544	1
Shorter	Obst.	41	0.982	0.303, 1.208	1
	Loc.	41	1.602	1.231, 1.683	1
Taller	Obst.	45	0.976	0.417, 1.194	1
	Loc.	46	1.684	1.349, 1.828	1
Lower weight	Obst.	40	0.857	0.214, 1.098	1
	Loc.	40	1.643	1.246, 1.804	1
Higher weight	Obst.	46	1.048	0.517, 1.234	1
	Loc.	47	1.801	1.393, 2.000	1
Younger	Obst.	44	1.108	0.531, 1.352	1
	Loc.	44	1.658	1.289, 1.758	1
Older	Obst.	44	0.930	0.268, 1.155	1
	Loc.	43	1.761	1.390, 1.953	1

† The first line represents integration in the whole sample. Each subsequent set of results divides the whole sample into height, weight, and age groups, respectively.

Table 6. Allometric relationships with height.

Measurement	R^2	Relationship†	Slope (95% CI)
PUBC to AIIS (n=80)	0.216	-	0.578 (0.330, 0.826)
PMPS to AMPS (n=88)	0.048	isometry	0.846 (0.042, 1.650)
IPS to ISP (n=87)	0.273	-	0.580 (0.376, 0.784)
IPS to INN (n=87)	0.115	-	0.543 (0.218, 0.867)
IPS to INFT (n=87)	0.099	-	0.505 (0.176, 0.835)
IPS to MP4 (n=72)	0.094	-	0.404 (0.105, 0.702)
IPS to STIP (n=83)	0.060	-	0.328 (0.042, 0.614)
MSSPR to MISPR (n=87)	0.107	isometry	0.894 (0.336, 1.452)
MSIPR to MIIPR (n=87)	0.086	isometry	0.860 (0.256, 1.465)
ISP to LSCI (n=87)	0.114	isometry	1.634 (0.650, 2.618)
ISP to SCI (n=67)	0.132	isometry	0.774 (0.283, 1.266)
INN to INN (n=87)	0.063	-	0.519 (0.086, 0.952)
INN to MP4 (n=72)	0.129	-	0.571 (0.218, 0.923)
POF to AOF (n=88)	0.086	-	0.468 (0.140, 0.796)
ACP to ACA (n=87)	0.201	-	0.533 (0.304, 0.762)
ACS to ACI (n=86)	0.290	-	0.615 (0.406, 0.824)
FHPROX to FHD (n=87)	0.330	-	0.723 (0.500, 0.945)
FHA to FHPOS (n=87)	0.306	-	0.729 (0.492, 0.966)
GTT to GTT (n=86)	0.191	-	0.585 (0.324, 0.847)
NA to NP (n=88)	0.180	-	0.633 (0.343, 0.923)

† - : negative allometric relationship; + : positive allometric relationship

Table 7. Allometric relationships with weight

Measurement	R^2	Relationship†	Slope (95% CI)
PUBC to AIIS (n=80)	0.051	-	0.064 (0.002, 0.125)
PMPS to AMPS (n=88)	0.050	-	0.199 (0.014, 0.385)
SPS to IPS (n=88)	0.059	-	0.128 (0.018, 0.237)
IPS to MP4 (n=72)	0.072	-	0.079 (0.011, 0.146)
IPS to STIP (n=83)	0.114	-	0.105 (0.040, 0.169)
LSSPR to LISPR (n=87)	0.065	-	0.219 (0.041, 0.398)
MSSPR to MISPR (n=87)	0.075	-	0.173 (0.042, 0.304)
MSIPR to MIIPR (n=87)	0.115	-	0.227 (0.091, 0.362)

ISP to SCI (n=67)	0.066	-	0.125 (0.008, 0.242)
INN to MP4 (n=72)	0.057	-	0.085 (0.003, 0.167)
FHPROX to FHD (n=87)	0.048	-	0.064 (0.003, 0.125)
† - : negative allometric relationship; + : positive allometric relationship			

Table 8. Scaling relationships with age			
Measurement	R^2	Relationship†	Slope (95% CI)
SPS to IPS (n=90)	0.180	-	0.120 (0.066, 0.174)
IPS to INFT (n=89)	0.052	-	-0.045 (-0.085, -0.004)
BISPP to BISPA (n=89)	0.065	-	0.145 (0.027, 0.263)
INN to INN (n=89)	0.084	-	-0.075 (-0.127, -0.022)
INFT to INFT (n=89)	0.083	-	-0.068 (-0.116, -0.020)
ACP to ACA (n=89)	0.103	-	0.047 (0.017, 0.076)
ACS to ACI (n=88)	0.052	-	0.032 (0.003, 0.061)
FHPROX to FHD (n=89)	0.044	-	0.033 (0.000, 0.065)
† - : decreasing proportional relationship; + : increasing proportional relationship			

Figure legends

Figure 1.
Correlation plot of all measurements. Correlations outlined in red are correlations between locomotor measurements, while correlations outlined in blue are correlations between obstetric measurements. Most strong correlations occur within these subsets. The cluster of weak correlations outlined in purple are correlations between obstetric and locomotor measurements. Only statistically significant correlations are shown. This correlation plot was constructed using R version 3.4.2 (R Core Team, 2017) software package *corrplot* version 0.84 (Wei & Simko, 2017).

Figure 2.
(a) Plot showing the scaled magnitude of integration in obstetric (1.523 [1.241,1.546]) and locomotor (1.987 [1.705, 2.060]) measurements in the whole sample, excluding measurements associated with intra-observer error. Locomotor measurements are more highly integrated than obstetric measurements, and the confidence intervals do not overlap.
(b) Plot showing the scaled magnitude of integration in obstetric (1.392 [0.784, 1.716]) and locomotor (2.408 [2.109, 2.544]) measurements in the pubis in the whole sample. Locomotor measurements were more highly integrated than obstetric measurements, and the confidence intervals do not overlap. Pubic obstetric confidence intervals fall below 1.

Filled circles represent scaled $SD_{rel}(\boldsymbol{\lambda})$, lines and bars represent 95% confidence intervals calculated using a bootstrap method, and unfilled circles represent expected values of scaled $SD_{rel}(\boldsymbol{\lambda})$if measurements were unintegrated, which equals one.

Figure 3.
(a) Plot showing the scaled magnitude of integration in obstetric and locomotor measurements in shorter (obstetric: 1.085 [0.721, 1.100] locomotor: 1.223 [0.871, 1.246]) and taller (obstetric: 1.182 [0.890, 1.157] locomotor: 1.374 [1.076, 1.408]) women, excluding measurements associated with intra-observer error. Obstetric and locomotor confidence intervals overlap within and between both groups. Obstetric and locomotor confidence intervals fall below 1 in shorter women, and obstetric confidence intervals fall below 1 in taller women.
(b) Plot showing the scaled magnitude of integration in obstetric and locomotor measurements in the pubis in shorter (obstetric: 0.982 [0.303, 1.208] locomotor: 1.602 [1.231, 1.683]) and taller (obstetric: 0.976 [0.417, 1.194] locomotor: 1.684 [1.349, 1.828]) women. Locomotor integration is higher than obstetric integration in both groups, with no confidence interval overlap. There is no significant difference between groups. Obstetric integration falls below 1 in both groups, but confidence intervals include 1.
Filled circles represent scaled $SD_{rel}(\boldsymbol{\lambda})$, lines and bars represent 95% confidence intervals calculated using a bootstrap method, and unfilled circles represent expected values of scaled $SD_{rel}(\boldsymbol{\lambda})$ if measurements were unintegrated, which equals one.

Figure 4.
Scatterplots of allometric relationships with height. In (a), as height increases, IPS to ISP increases as well. The proportional relationship between IPS to ISP and height decreases, such that IPS to ISP is relatively larger at shorter heights. In (b), as height increases, ISP to SCI increases, and ISP to SCI increases in constant proportion with height. In (c), the scaling is the same as in (a). Allometry scatter plots were constructed using an R function published by (Raviv, 2015).
(a) The negative allometric relationship between IPS to ISP and height (R^2 = 0.273, slope = 0.580 [0.376, 0.784]).
(b) The isometric relationship between ISP to SCI and height (R^2 = 0.132, slope = 0.774 [0.283, 1.266]).
(c) The negative allometric relationship between FHA to FHPOS and height R^2 = 0.306, slope = 0.729 [0.492, 0.966]).

Figure 5.
(a) Plot showing the scaled magnitude of integration in obstetric and locomotor measurements in lower weight (obstetric: 1.086 [0.768, 1.060] locomotor: 1.379 [1.058, 1.429]) and higher weight (obstetric: 1.215 [0.902, 1.232] locomotor: 1.445 [1.090, 1.517]) women, excluding measurements associated with intra-observer error. Locomotor confidence intervals just overlap with obstetric confidence intervals in lower weight women and overlap in higher weight women. There is no significant difference between the groups. Obstetric confidence intervals fall below 1 in both groups.
(b) Plot showing the scaled magnitude of integration in obstetric and locomotor measurements in the pubis in lower weight (obstetric: 0.857 [0.214, 1.098] locomotor: 1.643 [1.246, 1.804]) and higher weight (obstetric: 1.048 [0.517, 1.234] locomotor: 1.801 [1.393, 2.000]). Locomotor

measurements are more integrated than obstetric measurements in both groups, with no overlap in confidence intervals. There is no significant difference between the groups. Obstetric integration falls below 1 in lower weight women. Obstetric confidence intervals fall below 1 in both groups, but their confidence intervals include 1.
Filled circles represent scaled $SD_{rel}(\boldsymbol{\lambda})$, lines and bars represent 95% confidence intervals calculated using a bootstrap method, and unfilled circles represent expected values of scaled $SD_{rel}(\boldsymbol{\lambda})$ if measurements were unintegrated, which equals one.

Figure 6.
Scatterplots of allometric relationships with weight. In (a), as weight increases, IPS to STIP increases as well. The proportional relationship between IPS to STIP and weight decreases, such that IPS to STIP is relatively larger at lower weights. In (b) and (c), the scaling is the same as in (a). Allometry scatter plots were constructed using an R function published by (Raviv, 2015).
(a) The negative allometric relationship between IPS to STIP and weight (R^2 = 0.114, slope = 0.105 [0.040, 0.169])
(b) The negative allometric relationship between MSSPR to MISPR and weight (R^2 = 0.075, slope = 0.173 [0.042, 0.304])
(c) The negative allometric relationship between LSSPR to LISPR and weight (R^2 = 0.065, slope = 0.219 [0.041, 0.398])

Figure 7.
(a) Plot showing the scaled magnitude of integration in obstetric and locomotor measurements in younger (obstetric: 1.152 [0.837, 1.141] locomotor: 1.437 [1.080, 1.502]) and older (obstetric: 1.160 [0.848, 1.156] locomotor: 1.509 [1.208, 1.569]) women excluding measurements associated with intra-observer error. Obstetric and locomotor integration overlap in younger women but not older women. There was no difference between groups. Obstetric confidence intervals fall below 1 in both groups.
(b) Plot showing the scaled magnitude of integration in obstetric and locomotor measurements in the pubis in younger (obstetric: 1.108 [0.531, 1.352] locomotor: 1.658 [1.289, 1.758]) and older (obstetric: 0.930 [0.268, 1.155] locomotor: 1.761 [1.390, 1.953]) women. Obstetric and locomotor integration overlap in younger but not older women. There was no difference between the groups. Obstetric integration falls below 1 in older women, and obstetric confidence intervals fall below 1 and include 1 in both groups.
Filled circles represent scaled $SD_{rel}(\boldsymbol{\lambda})$, lines and bars represent 95% confidence intervals calculated using a bootstrap method, and unfilled circles represent expected values of scaled $SD_{rel}(\boldsymbol{\lambda})$ if measurements were unintegrated, which equals one.

Figure 8.
Scatterplots of scaling relationships with age. In (a), as age increases, SPS to IPS increases as well. The proportional relationship between SPS to IPS and age decreases, such that SPS to IPS is relatively larger at lower ages. In (b), the correlation is negative. The proportional relationship between INN to INN and age decreases, such that INN to INN is relatively larger at lower ages. Allometry scatter plots were constructed using an R function published by (Raviv, 2015).
(a) The negative scaling relationship between SPS to IPS and age (R^2 = 0.180, slope = 0.120 [0.066, 0.174])

(b) The negative scaling relationship between INN to INN and age (R^2 = 0.084, slope = -0.075 [-0.127, -0.022])

Figure 9.

Allometric relationships with height. Dashed lines represent negative allometry. Solid lines represent isometry. Lines and landmarks in blue represent obstetric measurements, while those in red represent locomotor measurements. Note that not all allometric relationships with height are represented in this figure.

(a) Anterior view

(b) Posterior view

Figure 10.

Allometric relationships with weight. Dashed lines represent negative allometry. Lines and landmarks in blue represent obstetric measurements, while those in red represent locomotor measurements. Note that not all allometric relationships with weight are represented in this figure.

(a) Anterior view

(b) Posterior view

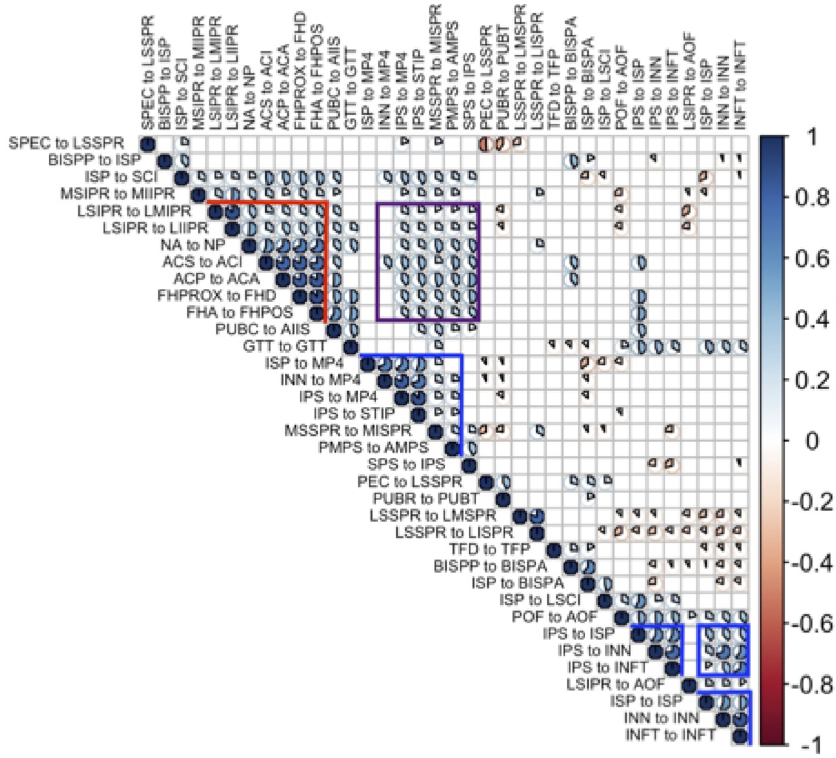

Figure 1.
Correlation plot of all measurements. Correlations outlined in red are correlations between locomotor measurements, while correlations outlined in blue are correlations between obstetric measurements. Most strong correlations occur within these subsets. The cluster of weak correlations outlined in purple are correlations between obstetric and locomotor measurements. Only statistically significant correlations are shown. This correlation plot was constructed using R version 3.4.2 (R Core Team, 2017) software package *corrplot* version 0.84 (Wei & Simko, 2017).

279x215mm (50 x 50 DPI)

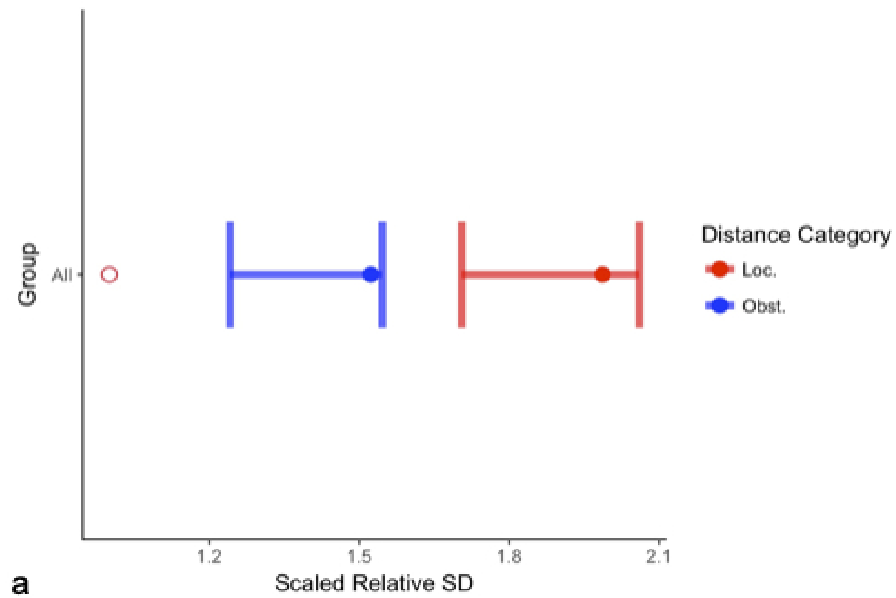

Figure 2.
(a) Plot showing the scaled magnitude of integration in obstetric (1.523 [1.241,1.546]) and locomotor (1.987 [1.705, 2.060]) measurements in the whole sample, excluding measurements associated with intra-observer error. Locomotor measurements are more highly integrated than obstetric measurements, and the confidence intervals do not overlap.

279x215mm (50 x 50 DPI)

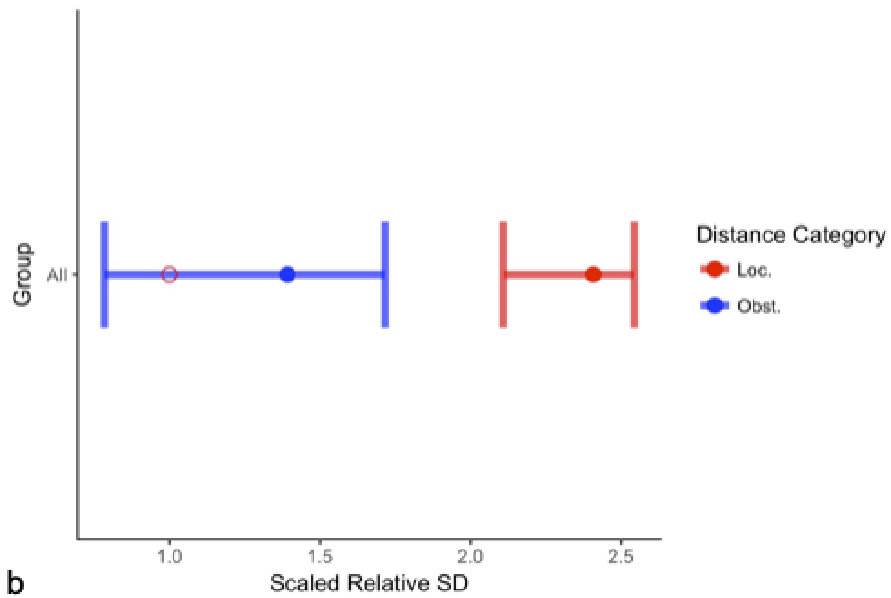

Figure 2. %"(b) Plot showing the scaled magnitude of integration in obstetric (1.392 [0.784, 1.716]) and locomotor (2.408 [2.109, 2.544]) measurements in the pubis in the whole sample. Locomotor measurements were more highly integrated than obstetric measurements, and the confidence intervals do not overlap. Pubic obstetric confidence intervals fall below 1. Filled circles represent scaled SD_{rel}(��), lines and bars represent 95% confidence intervals calculated using a bootstrap method, and unfilled circles represent expected values of scaled SD_{rel}(��)if measurements were unintegrated, which equals one.

279x215mm (50 x 50 DPI)

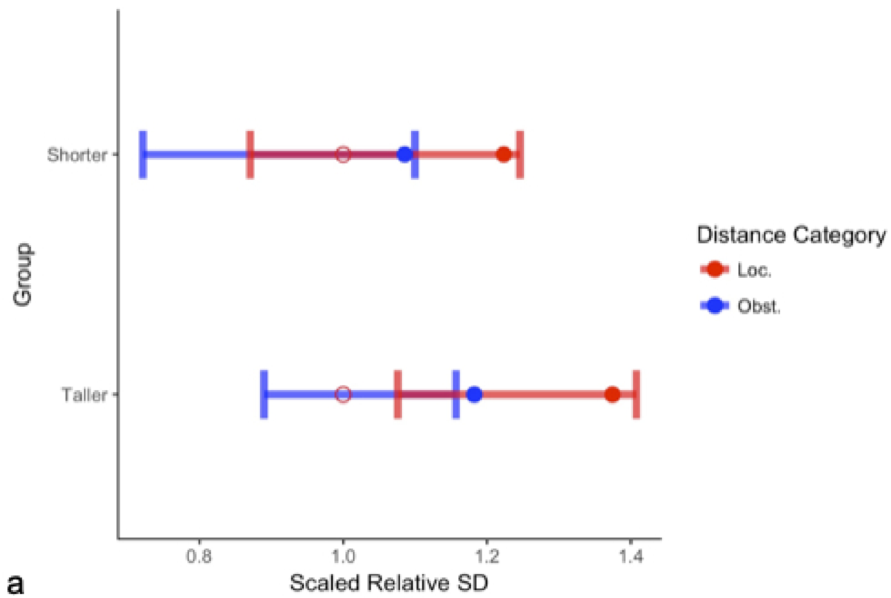

Figure 3.
(a) Plot showing the scaled magnitude of integration in obstetric and locomotor measurements in shorter (obstetric: 1.085 [0.721, 1.100] locomotor: 1.223 [0.871, 1.246]) and taller (obstetric: 1.182 [0.890, 1.157] locomotor: 1.374 [1.076, 1.408]) women, excluding measurements associated with intra-observer error. Obstetric and locomotor confidence intervals overlap within and between both groups. Obstetric and locomotor confidence intervals fall below 1 in shorter women, and obstetric confidence intervals fall below 1 in taller women.

279x215mm (50 x 50 DPI)

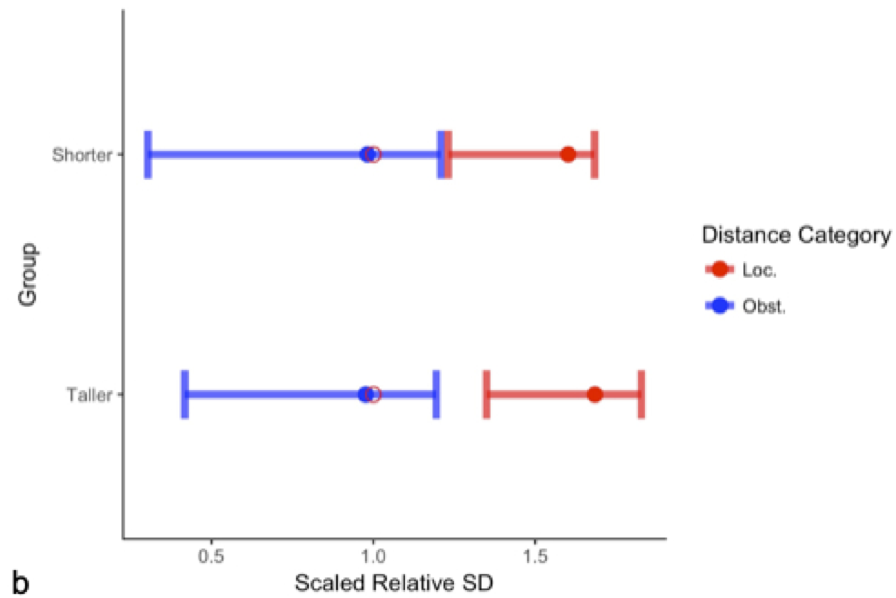

Figure 3.(b) Plot showing the scaled magnitude of integration in obstetric and locomotor measurements in the pubis in shorter (obstetric: 0.982 [0.303, 1.208] locomotor: 1.602 [1.231, 1.683]) and taller (obstetric: 0.976 [0.417, 1.194] locomotor: 1.684 [1.349, 1.828]) women. Locomotor integration is higher than obstetric integration in both groups, with no confidence interval overlap. There is no significant difference between groups. Obstetric integration falls below 1 in both groups, but confidence intervals include 1. Filled circles represent scaled SD_{rel}(��), lines and bars represent 95% confidence intervals calculated using a bootstrap method, and unfilled circles represent expected values of scaled SD_{rel}(��) if measurements were unintegrated, which equals one.

279x215mm (50 x 50 DPI)

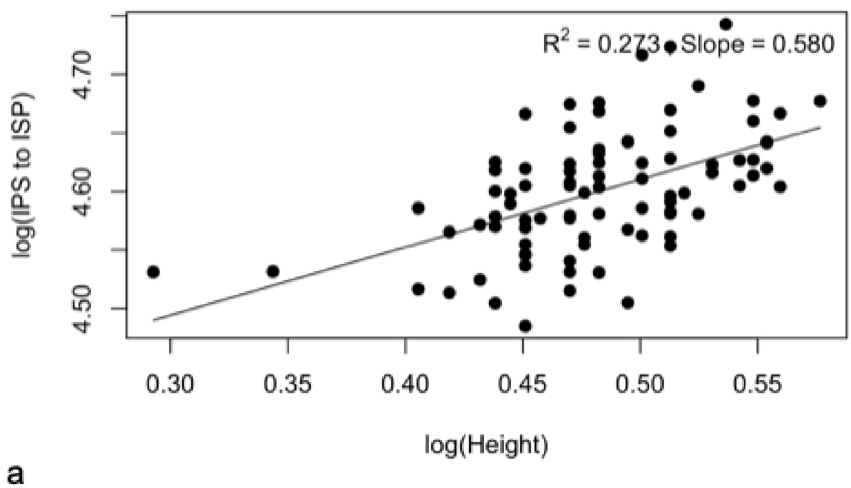

Figure 4. Scatterplots of allometric relationships with height. In (a), as height increases, IPS to ISP increases as well. The proportional relationship between IPS to ISP and height decreases, such that IPS to ISP is relatively larger at shorter heights. In (b), as height increases, ISP to SCI increases, and ISP to SCI increases in constant proportion with height. In (c), the scaling is the same as in (a).(a) The negative allometric relationship between IPS to ISP and height (R^2 = 0.273, slope = 0.580 [0.376, 0.784]).

279x215mm (50 x 50 DPI)

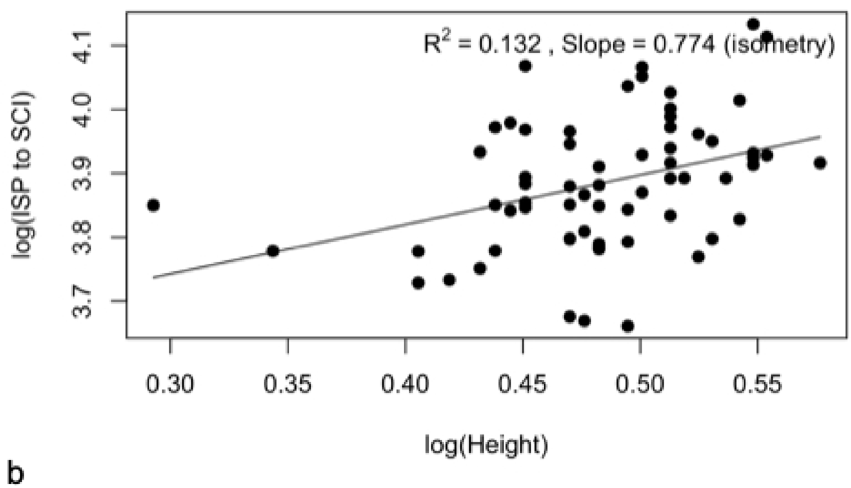

Figure 4. (b) The isometric relationship between ISP to SCI and height (R^2 = 0.132, slope = 0.774 [0.283, 1.266]).

279x215mm (50 x 50 DPI)

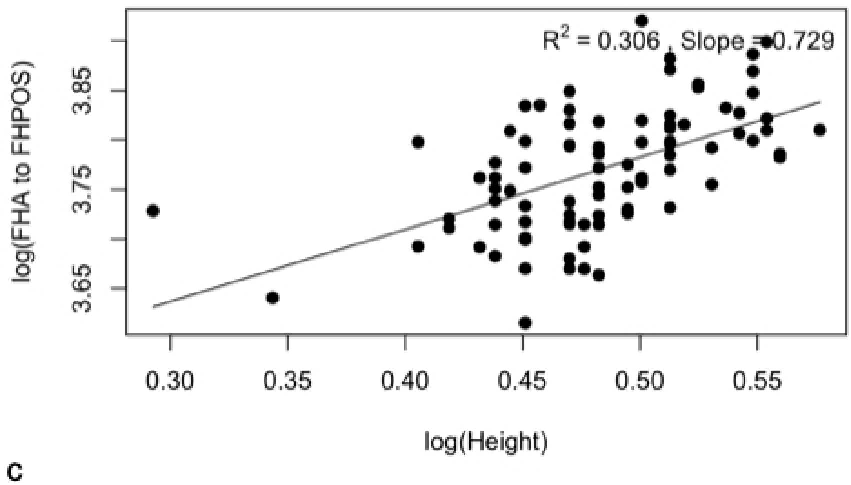

Figure 4. (c) The negative allometric relationship between FHA to FHPOS and height R^2 = 0.306, slope = 0.729 [0.492, 0.966]).

279x215mm (50 x 50 DPI)

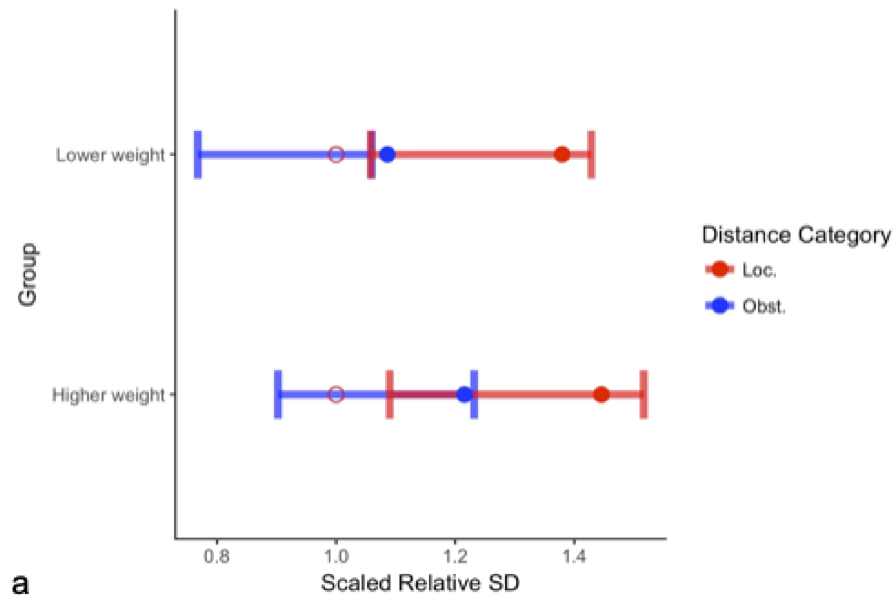

Figure 5.
(a) Plot showing the scaled magnitude of integration in obstetric and locomotor measurements in lower weight (obstetric: 1.086 [0.768, 1.060] locomotor: 1.379 [1.058, 1.429]) and higher weight (obstetric: 1.215 [0.902, 1.232] locomotor: 1.445 [1.090, 1.517]) women, excluding measurements associated with intra-observer error. Locomotor confidence intervals just overlap with obstetric confidence intervals in lower weight women and overlap in higher weight women. There is no significant difference between the groups. Obstetric confidence intervals fall below 1 in both groups.

279x215mm (50 x 50 DPI)

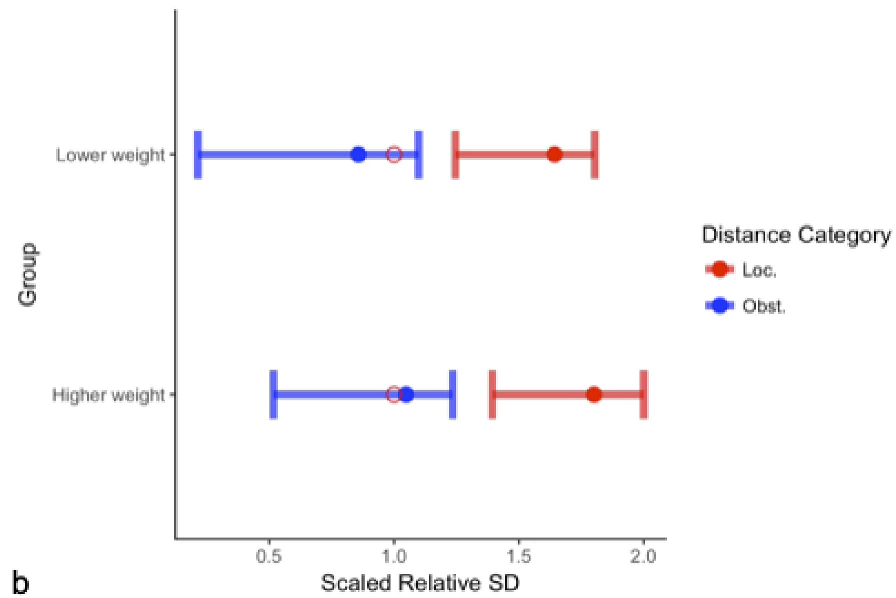

(b) Plot showing the scaled magnitude of integration in obstetric and locomotor measurements in the pubis in lower weight (obstetric: 0.857 [0.214, 1.098] locomotor: 1.643 [1.246, 1.804]) and higher weight (obstetric: 1.048 [0.517, 1.234] locomotor: 1.801 [1.393, 2.000]). Locomotor measurements are more integrated than obstetric measurements in both groups, with no overlap in confidence intervals. There is no significant difference between the groups. Obstetric integration falls below 1 in lower weight women. Obstetric confidence intervals fall below 1 in both groups, but their confidence intervals include 1. Filled circles represent scaled SD_{rel}(��), lines and bars represent 95% confidence intervals calculated using a bootstrap method, and unfilled circles represent expected values of scaled SD_{rel}(��) if measurements were unintegrated, which equals one.

279x215mm (50 x 50 DPI)

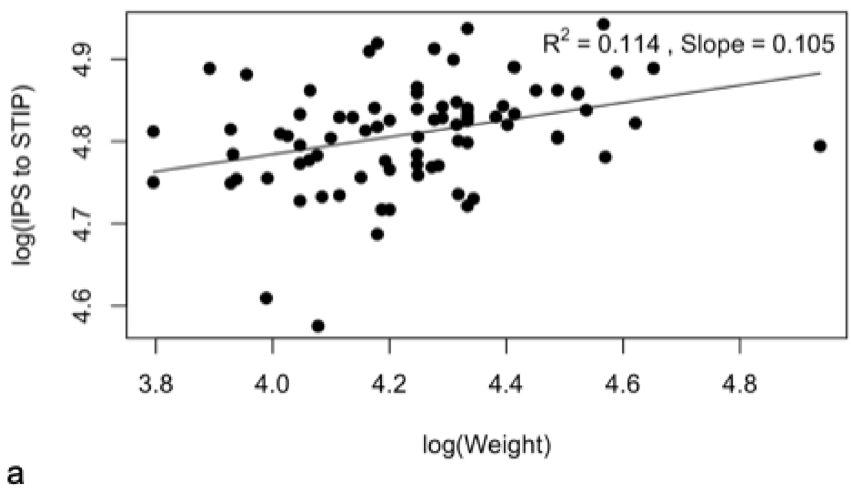

Figure 6. Scatterplots of allometric relationships with weight. In (a), as weight increases, IPS to STIP increases as well. The proportional relationship between IPS to STIP and weight decreases, such that IPS to STIP is relatively larger at lower weights. In (b) and (c), the scaling is the same as in (a).(a) The negative allometric relationship between IPS to STIP and weight (R^2 = 0.114, slope = 0.105 [0.040, 0.169])

279x215mm (50 x 50 DPI)

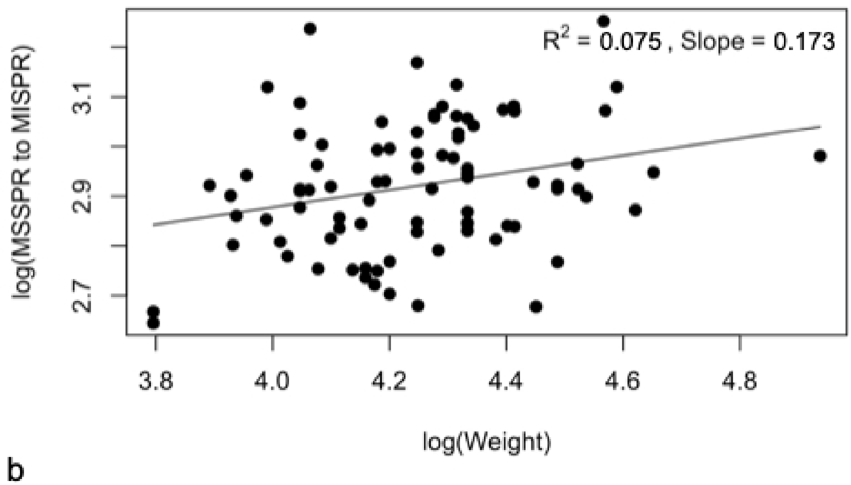

Figure 6. (b) The negative allometric relationship between MSSPR to MISPR and weight (R^2 = 0.075, slope = 0.173 [0.042, 0.304])

279x215mm (50 x 50 DPI)

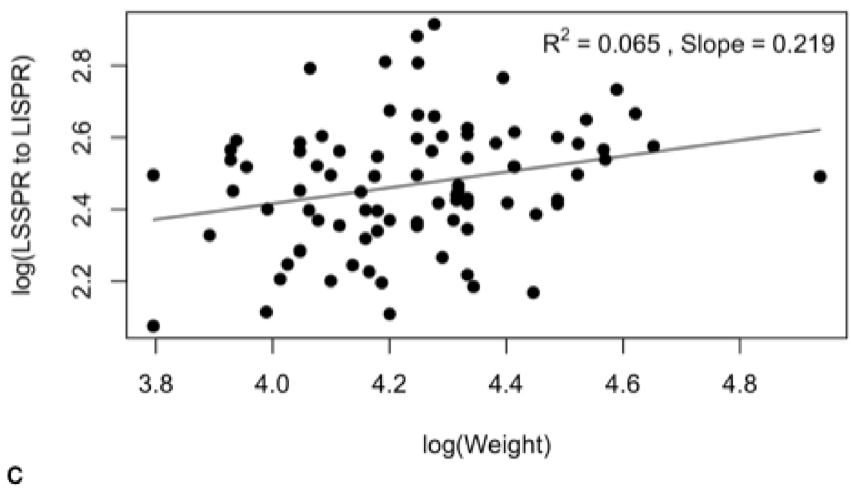

Figure 6. (c) The negative allometric relationship between LSSPR to LISPR and weight (R^2 = 0.065, slope = 0.219 [0.041, 0.398])

279x215mm (50 x 50 DPI)

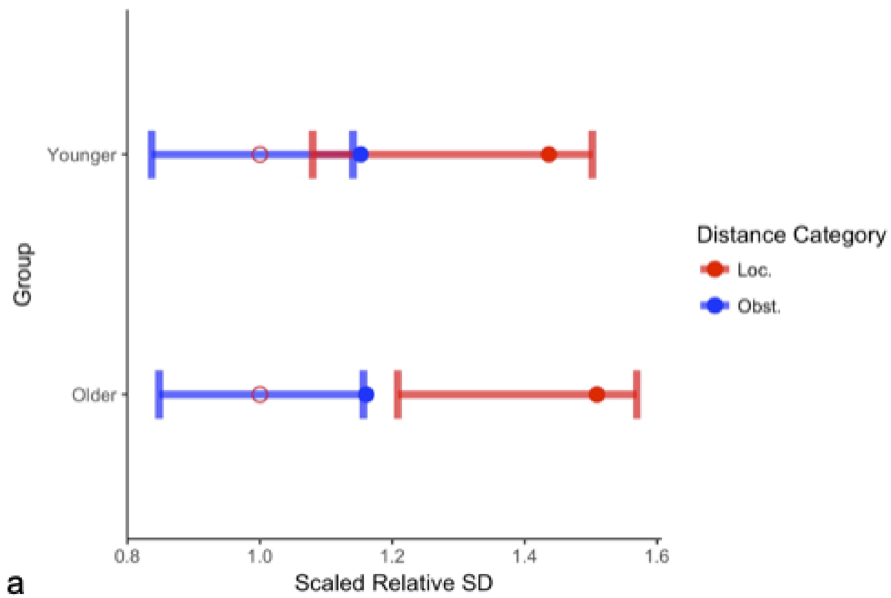

Figure 7.
(a) Plot showing the scaled magnitude of integration in obstetric and locomotor measurements in younger (obstetric: 1.152 [0.837, 1.141] locomotor: 1.437 [1.080, 1.502]) and older (obstetric: 1.160 [0.848, 1.156] locomotor: 1.509 [1.208, 1.569]) women excluding measurements associated with intra-observer error. Obstetric and locomotor integration overlap in younger women but not older women. There was no difference between groups. Obstetric confidence intervals fall below 1 in both groups.

279x215mm (50 x 50 DPI)

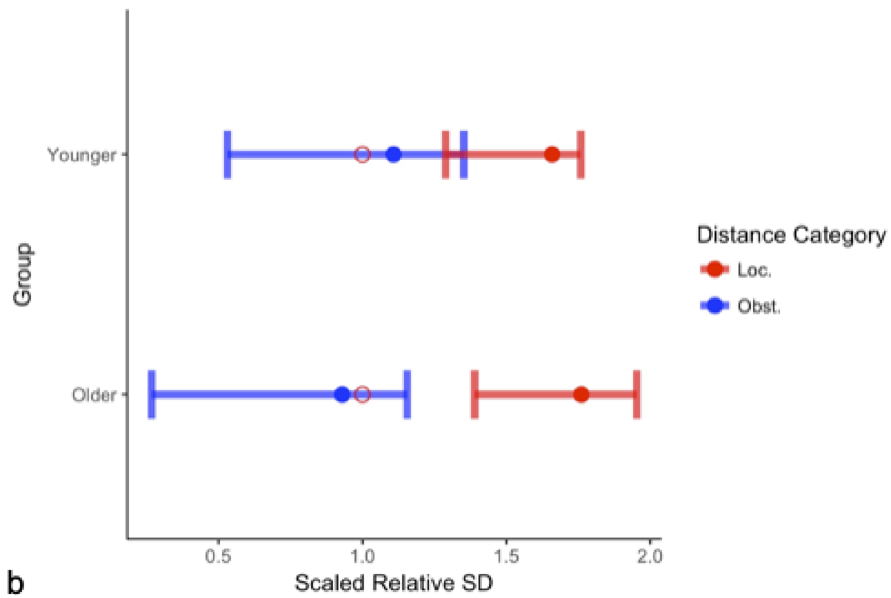

Figure 7. (b) Plot showing the scaled magnitude of integration in obstetric and locomotor measurements in the pubis in younger (obstetric: 1.108 [0.531, 1.352] locomotor: 1.658 [1.289, 1.758]) and older (obstetric: 0.930 [0.268, 1.155] locomotor: 1.761 [1.390, 1.953]) women. Obstetric and locomotor integration overlap in younger but not older women. There was no difference between the groups. Obstetric integration falls below 1 in older women, and obstetric confidence intervals fall below 1 and include 1 in both groups. Filled circles represent scaled SD_{rel}(��), lines and bars represent 95% confidence intervals calculated using a bootstrap method, and unfilled circles represent expected values of scaled SD_{rel}(��) if measurements were unintegrated, which equals one.

279x215mm (50 x 50 DPI)

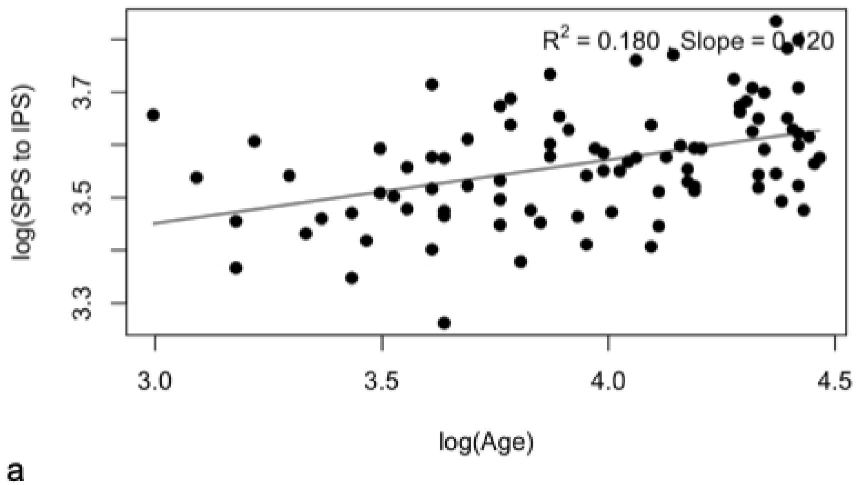

Figure 8. Scatterplots of scaling relationships with age. In (a), as age increases, SPS to IPS increases as well. The proportional relationship between SPS to IPS and age decreases, such that SPS to IPS is relatively larger at lower ages. In (b), the correlation is negative. The proportional relationship between INN to INN and age decreases, such that INN to INN is relatively larger at lower ages. (a) The negative scaling relationship between SPS to IPS and age (R^2 = 0.180, slope = 0.120 [0.066, 0.174])

279x215mm (50 x 50 DPI)

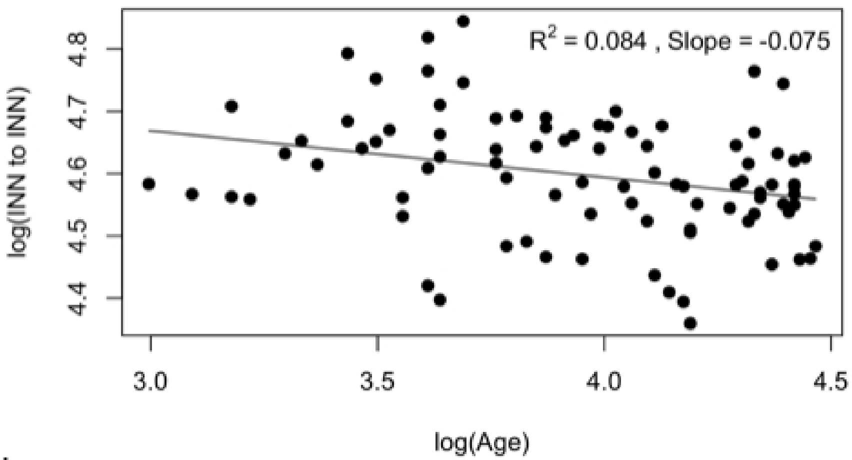

b

Figure 8. (b) The negative scaling relationship between INN to INN and age (R^2 = 0.084, slope = -0.075 [-0.127, -0.022])

279x215mm (50 x 50 DPI)

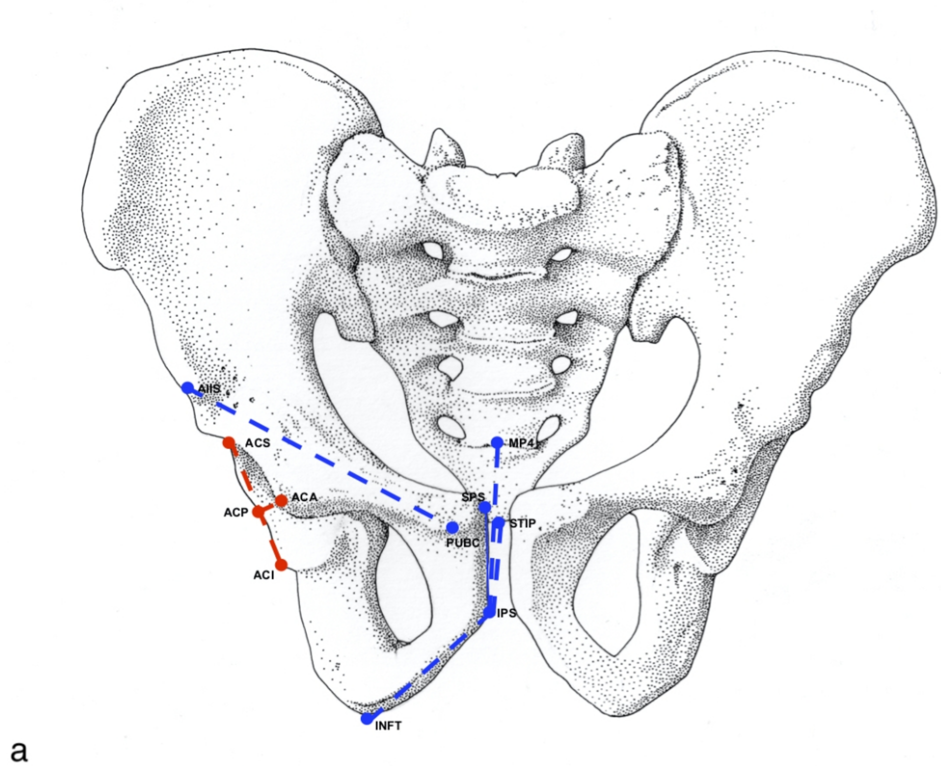

Figure 9.
Allometric relationships with height. Dashed lines represent negative allometry. Solid lines represent isometry. Lines and landmarks in blue represent obstetric measurements, while those in red represent locomotor measurements. Note that not all allometric relationships with height are represented in this figure.
(a) Anterior view

200x154mm (150 x 150 DPI)

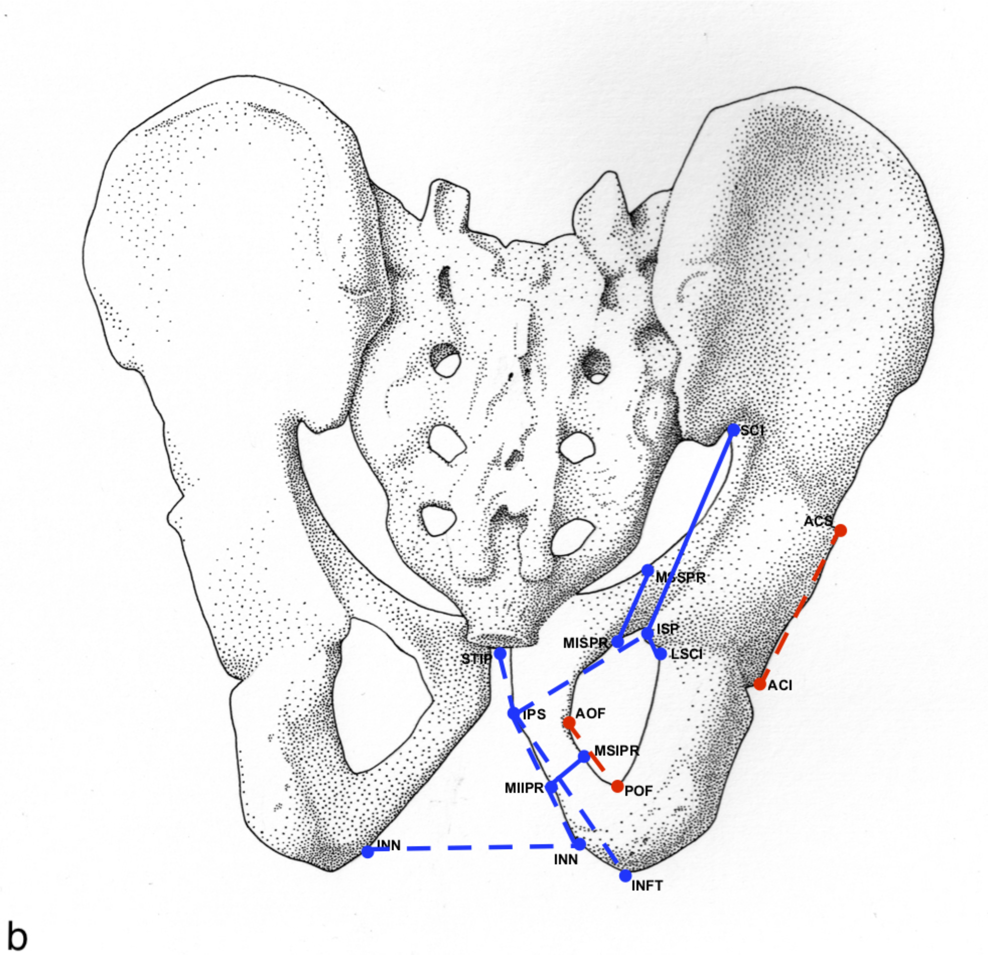

Figure 9.
(b) Posterior view

168x161mm (150 x 150 DPI)

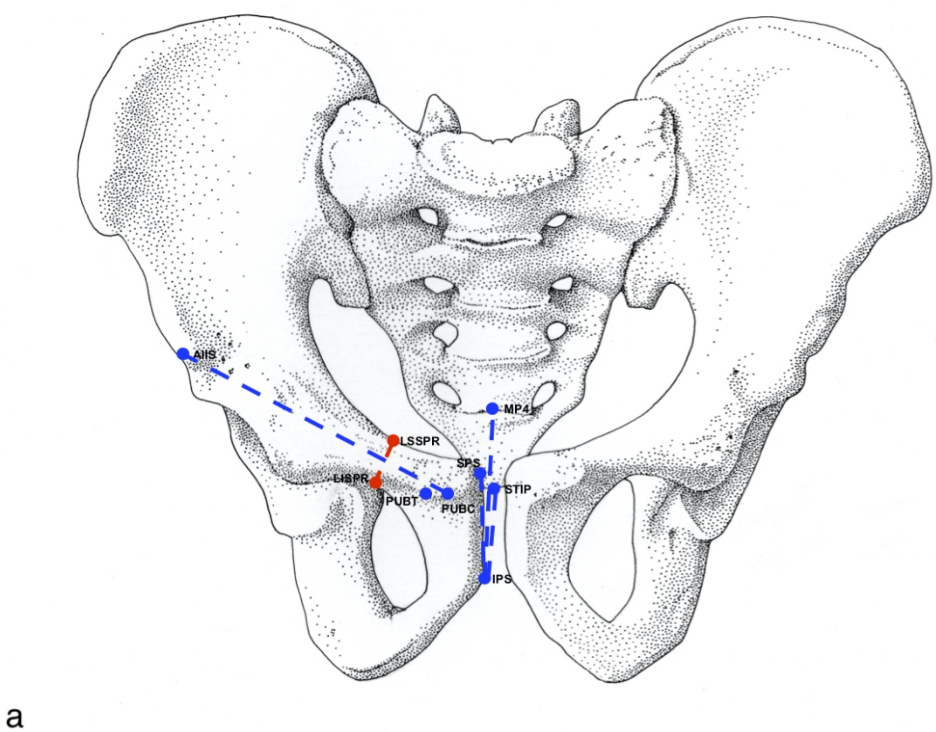

Figure 10.
Allometric relationships with weight. Dashed lines represent negative allometry. Lines and landmarks in blue represent obstetric measurements, while those in red represent locomotor measurements. Note that not all allometric relationships with weight are represented in this figure.
(a) Anterior view

200x154mm (150 x 150 DPI)

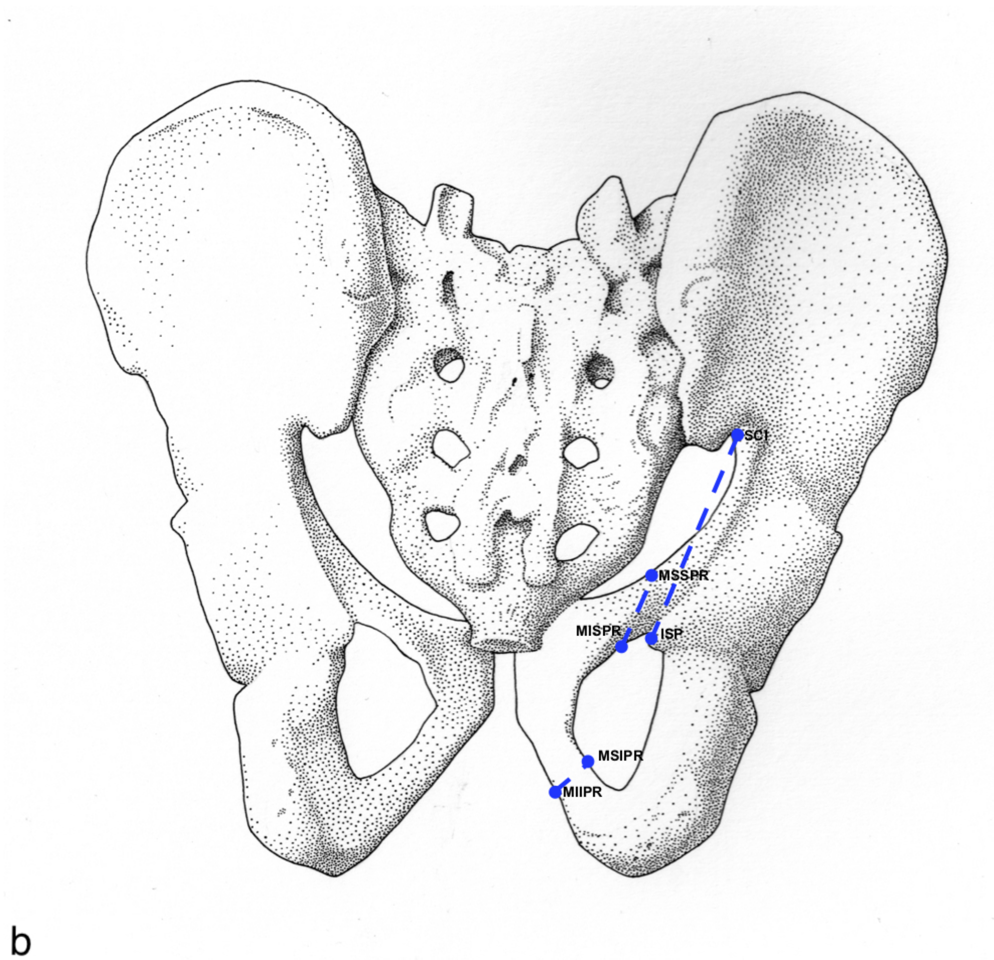

Figure 10.
(b) Posterior view

168x161mm (150 x 150 DPI)